Chemical and stable carbon isotopic compositions of $PM_{2.5}$ from two typical forests in China: Implication for sources

Mingyu Li[1], Zhanjie Xu[1*], Zhichao Dong[1], Junjun Deng[1], Pingqing Fu[1], Chandra Mouli Pavuluri[1*]

[1] Institute of Surface-Earth System Science, School of Earth System Science, Tianjin University, Tianjin 300072, China

Correspondance to: Zhanjie Xu (xuzhanjie@tju.edu.cn); Chandra Mouli Pavuluri (cmpavuluri@tju.edu.cn)

Abstract. To elucidate the origin and seasonality of atmospheric aerosols in forest areas, simultaneous $PM_{2.5}$ collection was carried out in two typical forest sites: Changbai Mountain (CB, 42.40N, 128.11E), North China and Xishuangbanna (BN, 22.25N, 100.89E), South China, at day and night during the summer and winter periods of 2023-2024. Carbonaceous and nitrogenous components, water-soluble inorganic ions (WSII) and stable carbon isotopic composition of total carbon ($\delta^{13}C_{TC}$) were measured in $PM_{2.5}$. Generally, the contents of carbonaceous and nitrogenous components were higher in winter than in summer, with secondary organic carbon (SOC) and water-soluble organic carbon (WSOC) being higher in daytime than that in nighttime at both CB and BN. The average concentrations of WSII in total samples were 5.36 μg m^{-3} and 2.23 μg m^{-3} at CB and BN, respectively. SO_4^{2-}, NO_3^- and NH_4^+ were dominant at CB, while SO_4^{2-}, NH_4^+ and Na^+ were dominant at BN, which accounted for 86% and 89% in BN to the total ions, respectively. $\delta^{13}C_{TC}$ ranged from −27.8‰ to −22.1‰ at CB, while −27.6‰ to −24.5‰ at BN. Besides biogenic emissions, the emissions from biomass burning and terrestrial and/or marine organisms were major sources of aerosols at both sites. Furthermore, fossil fuel combustion contributed more significantly at CB than at BN in winter. This study sheds better light on the seasonality in chemical composition and origins of $PM_{2.5}$ in forest areas in North and South China.

1 Introduction

Fine aerosols are the particulate matter with an aerodynamic diameter less than or equal to 2.5 μm ($PM_{2.5}$) in the atmosphere. $PM_{2.5}$ can influence the Earth's climate system through solar radiation absorption or scattering, and indirectly by acting as cloud condensation nuclei (Liou and Ou, 1989; Ramana and Devi, 2016). In addition, $PM_{2.5}$ has been found to have adverse impacts on visibility, human health and ecosystems (Shaughnessy et al., 2015; Maji et al., 2018; Zhang et al., 2019; Xue et al., 2022; Chen et al., 2023; Zheng et al., 2024). Furthermore, recent studies have found that $PM_{2.5}$ affects the productivity and aggravates socio-economic inequality (Peeples, 2020; Canaday et al., 2024; Li et al., 2024).

$PM_{2.5}$ consists mainly of water-soluble inorganic ions (WSII), carbonaceous components and trace elements (Wang et al., 2017; Zhao et al., 2022). Among them, WSII account for about 20-60% of $PM_{2.5}$ and their proportion increases with increasing pollution levels (Cao et al., 2007; Tao et al., 2014; Yin et al., 2014; He et al., 2017; Guo et al., 2023). Carbonaceous components primarily consist of elemental carbon (EC) and organic carbon (OC). EC originates mainly from incomplete combustion of

删除了: s
删除了: summer, with secondary organic carbon (SOC) and water-soluble organic carbon (WSOC) higher in daytime than in
删除了: during the
删除了: at
删除了: both
删除了: s
删除了: ab
删除了: Based on results obtained, we found that besides
删除了: the
删除了: Further fossil fuel combustion contributed more significantly at CB than at BN.
删除了: Thus, this
删除了: chemical
删除了: variations
删除了: and aging processes
删除了: that does not exceed
删除了: The
删除了: direct
删除了: serving
删除了: harmful
删除了: Further the recent studies found that the $PM_{2.5}$ affects the productivity and aggravates socio-economic inequality
设置了格式: 下标
删除了: s
删除了: s
删除了:
设置了格式: 非上标/ 下标

biomass and fossil fuels (Sharma et al., 2022). While OC is derived from primary organic matter directly released as particulate matter from pollution sources and by secondary formation from anthropogenic or biogenic emissions of volatile organic compounds (VOCs) (Ehn et al., 2014). Notably, WSII promote the formation of secondary organic aerosols (SOA) (Pathak et al., 2003; Fu et al., 2024). However, tracing the sources clearly by measuring only the chemical components in $PM_{2.5}$ is difficult. In recent studies, the stable carbon isotope ratios of total carbon ($\delta^{13}C_{TC}$) have been proven to aid in identifying the sources and transformation processes of $PM_{2.5}$ (Kawamura et al., 2004; Aggarwal et al., 2013; Kunwar et al., 2016; Pavuluri et al., 2011b).

Recent research on the sources of $PM_{2.5}$ has been extensively conducted worldwide (Kawashima et al., 2023; Espina-Martin et al., 2024; Chen et al., 2025). Therefore, comprehensive chemical composition studies of $PM_{2.5}$ from different regions remain important. Chinese studies on atmospheric $PM_{2.5}$ are predominantly focused on large and medium-sized cities and other regions with substantial populations or severe pollution, like the Beijing-Tianjin-Hebei urban agglomeration and the Yangtze River Delta. (Huang et al., 2014; Wang et al., 2021; Dong et al., 2023; Li et al., 2024). Nevertheless, due to variations in pollution sources, climate, geographical location, and other factors in different regions, the characteristics of $PM_{2.5}$ concentration and its chemical composition differ in various areas. Compared with urban areas, the composition of aerosols in forest regions are complex due to larger contributions of natural source components and their secondary formation and aging mechanisms make them more complicated (Bhat and Fraser, 2007; Mo et al., 2015; Ren et al., 2019; Ehn et al., 2014; Kourtchev et al., 2009). Forest plants act as major sources of biogenic VOCs, which serve as crucial precursors to $PM_{2.5}$, and can form biogenic SOA through photochemical reactions (Yuan et al., 2013; Wu et al., 2020). Furthermore, biomass burning is also a significant source of organic aerosol (OA), during which significant quantities of VOCs and particulate matter are emitted. These substances undergo a series of intricate chemical transformations, resulting in substantial OA formation (Long et al., 2023). This can seriously affect air quality, inducing marked elevations in $PM_{2.5}$ mass concentrations and posing a threat to public health (Bu et al., 2021; Chen et al., 2024; Yin et al., 2024). Therefore, research on the characterization and origin of aerosols in forest areas is necessary.

China has a vast land with a forest coverage of 24.02% in 2022. Therefore, we selected two typical forest areas that covered with different types of vegetation and located in the southern and northern China, representing the temperate and tropical zones of China, respectively, for this study. Here, we report the temporal variability in the concentrations and compositions of carbonaceous components, WSII, nitrogenous components, as well as $\delta^{13}C_{TC}$ of $PM_{2.5}$ at each site. Based on the data obtained, we explore the origins and aging processes of $PM_{2.5}$ in the forest regions in China.

2 Methodology

2.1 $PM_{2.5}$ Sampling

$PM_{2.5}$ sampling was performed at two forest sites: (i) the Changbai Mountain Forest Ecosystem Positioning Research Station of the Chinese Academy of Sciences (CB) in Jilin Province, Northeastern China [42.40°N, 128.11°E, 740 m asl] and (ii) the

删除了: human-made
删除了: s
删除了: aerosols
设置了格式: 下标
删除了: The
删除了: has
删除了: in recent studies
删除了:)
设置了格式: 非突出显示
删除了: ; doi: 10.1029/2011JD015617
设置了格式: 非突出显示
删除了: Currently, research on the origins of $PM_{2.5}$ has been widely carried out worldwide
设置了格式: 下标
删除了: centered
删除了: the variations in pollution sources, climate, geographical location, and other factors in different background areas, the characteristics of $PM_{2.5}$ concentration and its chemical composition differ in various region
设置了格式: 下标
删除了: in
删除了: , so
删除了: are
删除了: extensive biomass burning emits
删除了: the
删除了: this study
删除了: h
删除了: north
删除了: the observation and chemical analysis of $PM_{2.5}$
删除了: s
删除了: set
删除了: of north and south
设置了格式: 下标
删除了: ,

Guanping Management Station of Xishuangbanna National Nature Reserve (BN) in Yunnan Province, Southwestern China [22.25°N, 100.89°E, 872 m asl]. The weather over CB, where mixed coniferous and deciduous broad-leaved forests predominate, is characterized by temperate monsoon climate with cold-dry winters and warm-humid summers. The winter atmospheric conditions are significantly influenced by northwest monsoon, resulting in distinct atmospheric pollutant transport over the CB region. The BN is situated in the tropical monsoon climate zone with year-round warm-humid conditions, featuring predominantly tropical rainforest vegetation with rich biodiversity, where minimal human activity due to remoteness from industrial regions maintains atmospheric conditions closer to natural background levels (Fig. 1).

Aerosol samples (n = 120) were collected on pre-combusted (450°C, 6 h) quartz membrane filters (405.3 cm^2) employing a high-volume air sampler operated at 1.0 m^3 min^{-1} in daytime (23:30-10:30 UTC) and nighttime (11:00-24:00 UTC) in summer from 22 July to 7 August 2022 and in winter from 26 December 2022 to 9 January 2023. Prior to and after sampling, blank samples were obtained by setting the filter membrane on the sampler and allowing it to remain for 5 minutes without air pumping. The filter membrane was immediately wrapped in aluminum foil, sealed in a plastic pouch, and stored away from light after sampling. All samples were preserved under -20°C conditions until analysis.

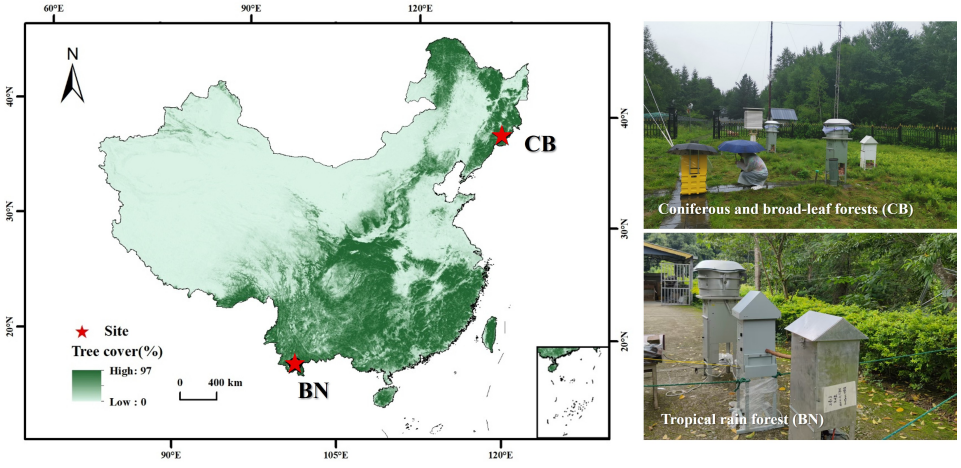

Figure 1: Map of China with the two sampling sites: Changbai Mountain (CB), North China and Xishuangbanna (BN), South China, with vegetation coverage.

删除了: its

删除了: , where mixed coniferous and deciduous broad-leaved forests predominate

删除了: and

删除了: pathways

删除了: ; and the Guanping Management Station of Xishuangbanna National Nature Reserve (BN) in Yunnan Province, Southwestern China [22.25°N, 100.89°E, 872 m asl],

删除了: The $PM_{2.5}$ samples (n = 120) were collected at the Changbai Mountain Forest Ecosystem Positioning Research Station of the Chinese Academy of Sciences (CB) in Jilin Province [42.40N, 128.11E, 740 m above sea level (asl)] and the Guanping Management Station of Xishuangbanna National Nature Reserve (BN) in Yunnan Province [22.25N, 100.89E, 872 m asl] (Fig. 1)

删除了: The filter membrane was enclosed in aluminum foil after every sampling, and put into a sealed plastic pouch, and stored away from light.

删除了: ↵

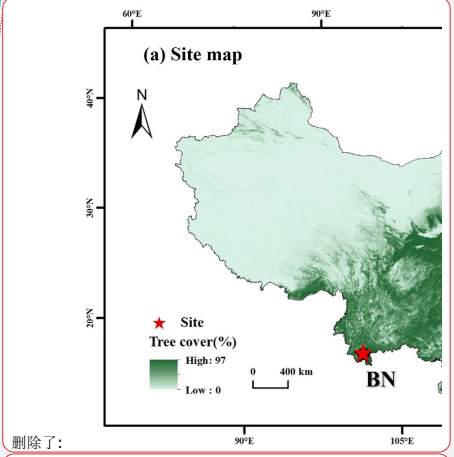

删除了:

删除了: (a)

删除了: points

删除了:

删除了: (b, c) Clustered 72-hour backward airmass trajectories plots (above the ground level: 500m) at CB and BN, China during 2023-24.

2.2 Chemical analyses

2.2.1 Measurement of carbonaceous components

The mass concentrations of OC and EC were measured using a semi-continuous thermal/optical OC/EC analyzer (Sunset Laboratory, USA). The distinction between OC and EC is achieved *via* real-time monitoring of light reflectance/transmittance changes during the heating process using a laser/light source, i.e. the IMPROVE protocol of the protective visual environment (Wan et al., 2017; 2015). Briefly, a portion of a filter was extracted and positioned in a quartz boat situated within the thermal desorption chamber, followed by combustion through a two-step heating procedure. Water-soluble OC (WSOC) was isolated from filter aliquots through ultrasonic extraction using Milli-Q water and quantified employing a TOC analyzer (OI Analytical, model 1030W C 1088). All measured concentrations were field blank-corrected to ensure data accuracy. The following equation was used to estimate the TC and water-insoluble OC (WIOC).

$$TC = OC + EC \quad (1)$$

$$WIOC = OC - WSOC \quad (2)$$

Owing to technical limitations in direct SOC determination, an EC tracer-based method was implemented for SOC assessment, which was estimated based on the following equation (Castro et al., 1999):

$$SOC = OC - [EC \times (OC/EC)_{min}] \quad (3)$$

where $(OC/EC)_{min}$ is the minimum value of the mass concentration ratio of OC/EC produced from primary emissions. Considering the differences in meteorological conditions and pollution source emissions at each sampling sites in different seasons, the average value of three $(OC/EC)_{min}$ monitored in different seasons at the sampling sites was applied to estimate the SOC. The minimum OC/EC ratios of 23.59, 7.15 in CB and 7.57, 17.26 in BN during the summer and winter, respectively.

2.2.2 Measurement of inorganic ions

The water-soluble ionic species (Cl^-, NO_3^-, SO_4^{2-}, Na^+, K^+, NH_4^+, Ca^{2+} and Mg^{2+}) were measured using Ion chromatography (ICS 5000+, Thermo Fisher). Briefly, an aliquot of a filter sample was ultrasonically extracted into 10 mL of Milli-Q water for 10 minutes (repeated 3 times). The extracts were then filtered through 0.22 μm Polytetrafluoroethylene (PTFE). To measure anions, an eluent consisting of Na_2CO_3, $NaHCO_3$, and H_2SO_4 was utilized at a controlled flow rate of 1.2 mL min^{-1}. For cation determination, methyl sulfonic acid functioned as the eluent, operating at a flow rate of 1.0 mL min^{-1} as described elsewhere (Dong et al., 2023; Pavuluri et al., 2011a). The concentrations of all ionic components were corrected for field blanks. Generally, the error in duplicate analyses did not exceed 4%. The nss-SO_4^{2-}, and nss-K^+ were calculated using Na^+ as a reference tracer for sea-salt correction (Tripathee et al., 2017).

It is worth noting that quartz filter membranes may interfere with certain specific cations (Na^+, Mg^{2+}, and Ca^{2+}). After measurement, it was found that the blank values (Na^+, Mg^{2+}, and Ca^{2+}) of the blank membranes at BN were relatively high,

删除了: 1

删除了: OC and EC were analyzed using a semi-continuous OC/EC analyzer (Sunset Laboratory, USA), which separates OC and EC by heating the sample at different temperatures and distinguishes between OC and EC by using a laser or light source to monitor changes in the reflected or transmitted light of the sample during the heating process.

删除了: analyzed

删除了: , which separates OC and EC by heating the sample at different temperatures

设置了格式: 字体: 倾斜

设置了格式: (中文) 中文(中国), (其他) 英语(美国)

删除了: ,

删除了: ,

删除了: ,

删除了: conducted

删除了: Inorganic ion analysis was conducted using Ion chromatography (ICS 5000+, Thermo Fisher). Briefly,

删除了: t

删除了: All t

设置了格式: 上标

设置了格式: 上标

设置了格式: 上标

设置了格式: 上标

设置了格式: 上标

while the measured concentrations of Mg^{2+}, and Ca^{2+} in the samples were very low. Therefore, the Ca^{2+} and Mg^{2+} at BN's samples were not discussed. The ion blank values of the blank membranes at CB site were all very low. Therefore, we believe that the influence on these cations can be negligible.

2.2.3 Measurement of nitrogenous components

Water-soluble total nitrogen (WSTN) was measured by a continuous-flow analyzer. The filter sample was ultrasonically extracted for 10 minutes in 10 mL of MilliQ water, repeated 3 times. The aqueous fractions were filtered using a 0.22 μm-sized PTFE membrane filter and subsequently mixed with excess K_2SO_4. The nitrogen (N) is converted to nitrate (NO_3^-) through ultraviolet digestion and then reduced to nitrite (NO_2^-). After that, the NO_2^- reacts with aminobenzene sulfonic acid to produce high molecular weight nitrogen compounds (Azo dye). Using a UV spectrophotometer to measure the total N's absorbance at 540 nm.

The inorganic nitrogen (IN) concentration was calculated by summing the measured concentrations of NO_2^--, NO_3^--, and NH_4^+-N. The concentration difference between WSTN and IN was regarded as water-soluble organic nitrogen (WSON) (Pavuluri et al., 2015; Dong et al., 2023).

$$[IN] = [NO_3^-\text{-N}] + [NH_4^+\text{-N}] + [NO_2^-\text{-N}] \quad (4)$$

$$[WSON] = [WSTN] - [IN] \quad (5)$$

2.2.4 Determination of stable carbon isotope ratios of TC

Stable carbon isotope ratios of TC ($\delta^{13}C_{TC}$) in $PM_{2.5}$ were analyzed through a Flash 2000HT elemental analyzer connected to a 253 Plus isotope ratio mass spectrometer (EA-IRMS). Overall, an aliquot of the filter was wrapped and injected into EA, with the evolved gases CO_2 delivered to an IRMS *via* ConFlo-II for the determination of $^{13}C/^{12}C$ in TC. The delta (δ) values represent the isotope ratio of $^{13}C/^{12}C$, in parts per million (ppm) with reference to Pee Dee Belemnite for carbon isotopes. The isotope conversion equation is as follows:

$$\delta^{13}C_{TC} = [(^{13}C/^{12}C)_{sample} / (^{13}C/^{12}C)_{standard} - 1] \times 1000 \quad (6)$$

The error derived from replicate analysis remains within 0.3‰. The samples were not decarbonized before measurement. Due to the fact that average Ca^{2+} concentrations were found to be low (0.03 ± 0.02 μg m^{-3}, CB; 0.09 ± 0.07 μg m^{-3}, BN) in these samples so that we assume that the contribution of $CaCO_3$ and its $\delta^{13}C$ to aerosols is negligible (Wang et al., 2005; Pavuluri et al., 2011b).

2.3 Meteorological parameters and simulations of air mass trajectories

Meteorological parameters, including temperature, relative humidity, and wind speed at CB and BN, were from the Xihe Energy Big Data Platform (https://xihe-energy.com/#geo). Considering the seasonal and diurnal variations in the planetary

删除了： A PTFE membrane filter with a 0.22 μm size was used to filter the aqueous fractions.
删除了: All
设置了格式: 非突出显示
设置了格式 ... [1]
删除了: digestion, and
设置了格式: 非突出显示
设置了格式 ... [2]
设置了格式 ... [3]
删除了: a
删除了: new nitrogen compounds
删除了: n
删除了: sample solution
设置了格式: 非突出显示
删除了: aggregating
设置了格式 ... [4]
设置了格式 ... [5]
设置了格式 ... [6]
删除了: ,
设置了格式 ... [7]
设置了格式 ... [8]
设置了格式 ... [9]
删除了: ,
删除了: io…os of TC ($\delta^{13}C_{TC}$) in $PM_{2.5}$ was ... [10]
删除了: ,
设置了格式: 下标
删除了:
设置了格式: 字体颜色: 自动设置, 英语(英国)

boundary layer (Wu et al., 2024). To analyze air mass transport patterns, 72-hour backward trajectories arriving at CB and BN at an altitude of 300 m, 500 m, and 1000 m above the ground level were calculated employing the Hybrid Single Particle Lagrangian Integrated Trajectory (HYSPLIT) model from the National Oceanic and Atmospheric Administration (https://www.ready.noaa.gov/index.php).

3 Results and discussion

3.1 Differences in meteorology and long-range transported air masses between the sampling sites

Figure 2 illustrates 72-hour backward air mass trajectory clusters. It revealed the air masses that reaching CB originated primarily from the Pacific Ocean, including the Yellow Sea and the East China Sea, while BN was primarily affected by the southwestern airflow from the Indian Ocean from the Bay of Bengal in summer. In winter, the air masses to CB were derived from North China and Mongolia. Compared with CB, the local source contribution at BN during winter was higher.

The temporal variations of meteorological parameters at two sites are depicted in Figure 2. The ambient temperatures at CB and BN during the campaigns exhibited seasonal variations. The temperatures at BN were similar to those at CB during summer, whereas in winter, the temperatures at BN (avg. 14.8°C) were significantly higher than those at CB (avg. -10.9°C). Both the pressure and wind speed were found to be higher at CB. Significant diurnal variations in relative humidity were observed at both sites, where CB demonstrated daytime and nighttime values of 84.84% and 72.03%, respectively, compared to BN's corresponding measurements of 90.84% and 73.96%.

设置了格式: 字体颜色: 自动设置, 英语(英国)
删除了: at 6-hour intervals
删除了: ↵
设置了格式: 字体: 非加粗, 字体颜色: 自动设置, 英语(英国)
设置了格式: 字体颜色: 自动设置, 英语(英国)
删除了: 1
删除了: (68%), the Sea of Japan (24%)
删除了: (8%)
删除了: , as well as airflows passing through the Indo-China Peninsula…
删除了: Siberia (51.0%)
删除了:
删除了: (30.0%)
删除了: (9.0%)
删除了: Fig. 2.
删除了: f
删除了:
删除了: the

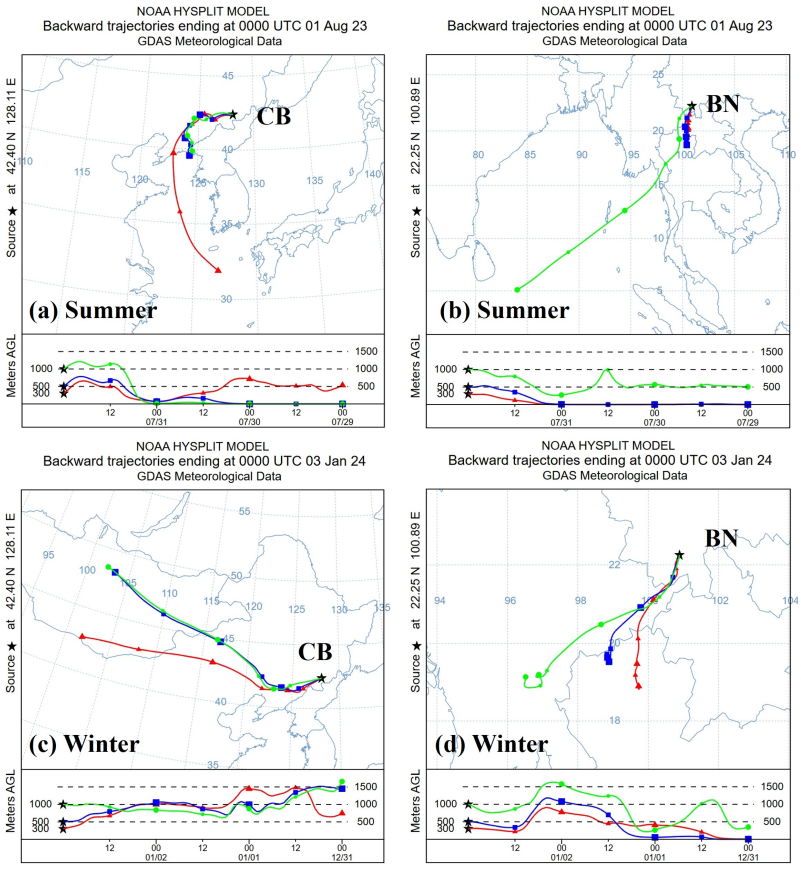

295 **Figure 2: Clustered 72-hour backward airmass trajectories plots (above the ground level: 300 m, 500 m, and 1000 m) at CB and BN, China during 2023-24.**

设置了格式: 字体: (中文) Times New Roman

设置了格式: 字体: (中文) Times New Roman, 字体颜色: 自动设置

带格式的: 题注

设置了格式: 字体: (中文) Times New Roman, 英语(英国)

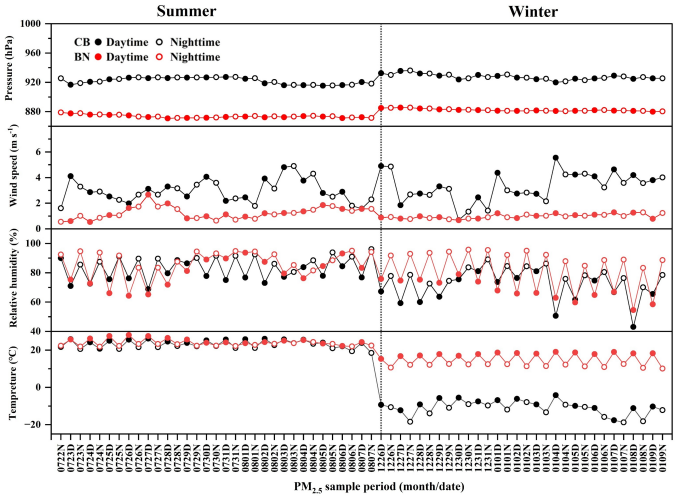

Figure 3: Temporal variations of meteorological parameters at CB and BN, China during 2023-24.

3.2 Chemical results

3.2.1 Characterization of inorganic ions and nitrogenous components

The linear regressions of total cations and anions were shown in Figure 4. The ratio of the equivalent concentrations of cation (CE) and anion (AE) can effectively evaluate the acid-base balance of aerosols (Tian et al., 2018). The formulas are as follows:

$$AE = \frac{Cl^-}{35.5} + \frac{SO_4^{2-}}{48} + \frac{NO_3^-}{62} \quad (7)$$

$$CE = \frac{Na^+}{23} + \frac{NH_4^+}{18} + \frac{K^+}{39} + \left(2*\frac{Mg^{2+}}{24}\right) + \left(2*\frac{Ca^{2+}}{40}\right) \quad (8)$$

If the CE is greater than the AE, $PM_{2.5}$ is alkaline, and *vice versa*. Average annual equivalent ratios of total cations (Na^+, NH_4^+, K^+, Mg^{2+} and Ca^{2+}) to anions (Cl^-, NO_3^- and SO_4^{2-}) were 1.62 ± 0.53 at CB and 1.92 ± 0.80 at BN, indicating that the aerosols at these two sites are alkaline. The high ratio of AE/CE might be due to the enhanced NH_3 emission caused by high temperature and agricultural activities (Qiao et al., 2019). It also should be noted that the excessive cations at both sites might be related to unmeasured anions like oxalate. Furthermore, soluble organic acid ions might also be the cause of the anion deficits at CB and BN. A more comprehensive investigation of this matter will be conducted in future research initiatives.

删除了: **2**

下移了 [1]: **Table 1: Annual and seasonal summary of concentrations of carbonaceous (EC, OC, SOC, WSOC and WIOC), nitrogenous (WSTN, IN and WSON) components and WSIIs (Cl^-, NO_3^-, SO_4^{2-}, Na^+, K^+, NH_4^+, Ca^{2+} and Mg^{2+}) (μg m^{-3}) and $\delta^{13}C_{TC}$ in $PM_{2.5}$ at CB and BN, China during 2023-24.**

删除了: ↵

删除了: Table 1 shows concentrations of carbonaceous (EC, OC, SOC, WSOC and WIOC), nitrogenous (WSTN, IN and WSON), WSIIs and $\delta^{13}C_{TC}$ in $PM_{2.5}$ at CB and BN, China in this study. ↵

带格式的: 标题 2

删除了: .g…re 43 … [11]

删除了: (Tian et al., 2018)

删除了: ,

设置了格式 … [12]

设置了格式 … [13]

设置了格式 … [14]

删除了: 2

删除了: 12

删除了: 2

删除了: 20...) , … [20]

设置了格式 … [15]

设置了格式 … [16]

设置了格式 … [17]

设置了格式 … [18]

设置了格式 … [19]

删除了: μg m^{-3}…atin…CB and 1.92 ± 0.80 μg m^{-3} …tin…BN, indicating that the aerosols at these two sites are alkaline. The high ratio of AE/CE might be due to the enhanced NH_3 emission caused by high temperature and agricultural activities (Qiao et al., 2019). It also should be noted that the excessive cations atin…both sites might be related to unmeasured anions like carbonate and …xalate. Furthermore, soluble organic acid ions might also be the cause of the anion deficits atin … [23]

设置了格式 … [21]

设置了格式 … [22]

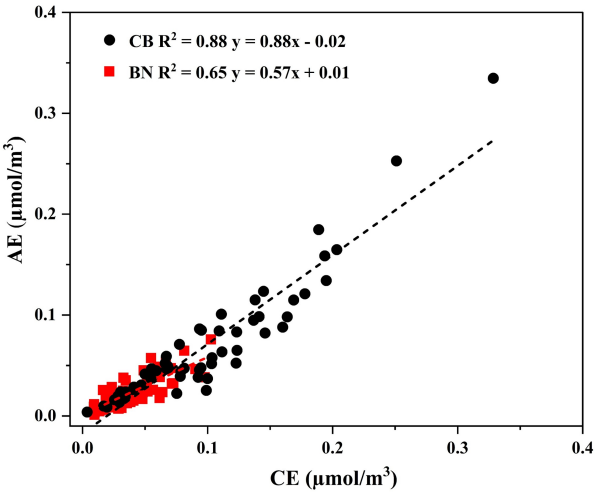

Figure 4: Anion and cation equilibrium in $PM_{2.5}$ collected from CB and BN.

Table S1 shows concentrations of carbonaceous (EC, OC, SOC, WSOC and WIOC) and nitrogenous (WSTN, IN and WSON) components, WSII, and $\delta^{13}C_{TC}$ in $PM_{2.5}$ at CB and BN, China in this study. For anions, SO_4^{2-} was identified as the predominant ionic species at both sites (CB: 2.31 μg m^{-3}; BN: 1.07 μg m^{-3}). They accounted for 43% and of total ionic mass at CB and 52% at BN, respectively. NO_3^- was the second abundant anion at both sites, followed by Cl^-. For cations, NH_4^+ was the most abundant ion (CB: 1.18μg m^{-3}; BN: 0.41μg m^{-3}) followed by Na^+, K^+, Mg^{2+} and Ca^{2+} at CB, whereas at BN, their abundances followed an order: $Na^+ > K^+ > Ca^{2+} Mg^{2+}$. As the main secondary ions in $PM_{2.5}$, the cumulative concentration SO_4^{2-}, NO_3^- and NH_4^+ reached 86% at CB and 76% at BN of the total ions, respectively. The concentrations of main secondary ions were significantly lower compared to those typically observed in urban sites, such as Tianjin, Beijing, Guangzhou, Chongqing in China, Chennai in India, and Hachinohe in Japan (Pathak et al., 2009; Qiao et al., 2019; Pavuluri et al., 2011a; Dong et al., 2023; Sun and Zhang, 2024). However, their concentrations were comparable to or even lower than those reported at rural background sites in France (Bressi et al., 2013), the southeastern United States (Nah et al., 2018), and at the forested site at K-puszta (Kourtchev et al., 2009). Except for Na^+ and K^+, The mean levels of different ions at CB exceeded those at BN. Ionic species exhibited peak concentrations in winter in their seasonal distributions (Fig. 5). However, the ionic species did not show a clear diurnal variation.

The concentrations of SO_4^{2-}, NH_4^+, and NO_3^- in $PM_{2.5}$ during winter were higher than those in summer, being 1.45, 2.55, and 73.00 times, respectively, at CB, and 2.57, 3.76, and 2.25 times, respectively, at BN. The coal combustion is considered as a major source of SO_2, NO_x, and NH_3 (Zhang et al., 2020; Zheng et al., 2022). The concentrations of secondary ions at CB were

删除了: ↵
删除了: 3
删除了: The concentration statistics of WSIIs in CB and BN $PM_{2.5}$ samples were shown in Table 1.
删除了: ,
带格式的: 制表位: 13.86 字符, 左对齐
删除了: s
删除了: On average,
删除了: .
删除了: second
设置了格式: 字体: (默认) +西文正文 (Times New Roman)
设置了格式: 字体: (默认) +西文正文 (Times New Roman)
设置了格式: 字体: (默认) +西文正文 (Times New Roman)
设置了格式: 字体: (默认) +西文正文 (Times New Roman)
删除了: NO_3^-,
删除了: Cl^-,
删除了: > NO_3^-
删除了: >Cl^- >
设置了格式: 字体: (默认) +西文正文 (Times New Roman)
设置了格式: 字体: (默认) +西文正文 (Times New Roman)
设置了格式: 字体: (默认) +西文正文 (Times New Roman)
删除了: Interestingly, NH_4^+ and Na^+ were the second and third abundant ions, in total ions at BN.
删除了: in
删除了:
删除了: 4
设置了格式: 字体颜色: 自动设置
下移了 [2]: Coal combustion is a major source of SO_2, NO_x, and NH_3 (Zhang et al., 2020; Zheng et al., 2022).
删除了:
删除了: ,
删除了:
删除了: ,
设置了格式: 字体: +西文正文 (Times New Roman)
设置了格式: 字体: +西文正文 (Times New Roman)
设置了格式: 字体: +西文正文 (Times New Roman)
设置了格式: 字体: +西文正文 (Times New Roman)
删除了: .
删除了: C
设置了格式: 非突出显示
删除了: Moreover, t

higher than that at BN in winter. This could be linked to the increased utilization of coal for domestic heating in winter, which leads to substantial emissions of gaseous precursors like SO_2 and NO_x. This also explains the rapid increase in NO_3^- concentrations during winter at CB. NO_3^- is primarily influenced by industrial and vehicular sources. Except during winter at CB, its concentrations remain consistently low, indicating minimal anthropogenic influence on forest sites. This was consistent with the concentrations reported by Tanner et al. (2004) for rural (avg. 0.04 μg m^{-3}) and background sites (avg. 0.01 μg m^{-3}) in the Tennessee Valley, USA, particularly during summer. Oceanic phytoplankton and/or dimethyl sulfide (DMS) emitted from biomass burning undergo photochemical oxidation to convert into SO_2, which subsequently transformed into SO_4^{2-} (Meinardi et al., 2003). However, Cl^- can also come from the oceanic emission, but its concentration was very low, indicating that SO_4^{2-} was not significantly affected by the oceanic emissions. This further implies the significance of anthropogenic sources. In addition, the low temperatures in winter resulted in a decreased atmospheric boundary layer, which hindered the dispersion of pollutants.

Figure 6 summarizes the concentrations and percentage contributions of various water-soluble ionic components. The contribution of NO_3^- to total ions at BN was very small in both summer (3%) and winter (3%), which may be attributed to the removal effect of wet deposition on nitrate particles due to the hot and humid climate throughout the year. However, the lower temperature environment (<15°C) in winter might facilitated the transformation of gaseous nitric (HNO_3) acid to particulate (NH_4NO_3), thereby potentially increasing the concentration of particulate NO_3^-. On the other hand, anthropogenic activities such as winter heating might emit more NOx, which, after undergoing a sequence of chemical reactions in the atmosphere, were converted into NO_3^-. Therefore, the contribution of NO_3^- (28%) in winter at CB was relatively high.

The average concentration of WSTN was 2.33 ± 2.34 μg m^{-3}, and IN was 1.85 ± 1.26 μg m^{-3} at CB, while 1.29 ± 0.51 μg m^{-3} and 0.52 ± 0.23 μg m^{-3} at BN. WSTN, IN, WSON and secondary ions had the same seasonal variation trend in concentration, with higher levels in winter (Fig. 7). WSON constituted an average of 57.7% of WSTN at CB and 40.3% at BN, respectively. WSON/WSTN at CB and BN were significantly higher as than other sites located in Himalaya (18%, hill site), New Delhi, India (19%, urban site), Sapporo, Japan (9%, urban site) and Svalbard Islands, Norway (8%, Coastal site) (Pavuluri et al., 2015; Tripathee et al., 2021; Boreddy et al., 2024; Pei et al., 2024). Similarities were noted with the forest aerosols collected from Rondônia, Brazil, during an intense biomass burning period. (~45%, forest site) (Mace et al., 2003).

删除了:
删除了:
设置了格式: 字体: (默认) +西文正文 (Times New Roman), 非倾斜
设置了格式: 字体: (默认) +西文正文 (Times New Roman), 非倾斜
删除了:
删除了:
设置了格式: 字体: +西文正文 (Times New Roman)
设置了格式: 字体: +西文正文 (Times New Roman)
移动了(插入) [3]
删除了: Additionally, O
删除了: .
删除了: their
设置了格式: 字体颜色: 自动设置
删除了: minimally
设置了格式: 字体颜色: 自动设置
删除了: A
删除了: a
删除了: ally
上移了 **[3]:** Oceanic phytoplankton and/or dimethyl sulfide (DMS) emitted from biomass burning undergo photochemical oxidation to convert into SO_2, which subsequently transformed into SO_4^{2-}.
删除了: The consistently higher concentrations of SO_4^{2-} at CB might be associated with CB's proximity to the coast.
删除了: 5
设置了格式: 字体: (默认) +西文正文 (Times New Roman), 非倾斜
设置了格式: 字体: (默认) +西文正文 (Times New Roman), 非倾斜
设置了格式: 字体: (默认) +西文正文 (Times New Roman), 非倾斜
删除了: In addition, the higher contribution of Na^+ (25%) and the very low contribution of Mg^{2+} (about 0%) at BN during summer implies that the Na^+ could have been originated primarily from marine emissions rather than from soil dust.
删除了: 6
删除了: Table 1: Annual and seasonal summary of concentrations of carbonaceous (EC, OC, SOC, WSOC and WIOC), nitrogenous (WSTN, IN and WSON) components and WSIIs (Cl^-, NO_3^-, SO_4^{2-}, Na^+, K^+, NH_4^+, Ca^{2+} and Mg^{2+}) (μg m^{-3}) and $\delta^{13}C_{TC}$ in $PM_{2.5}$ ... [24]

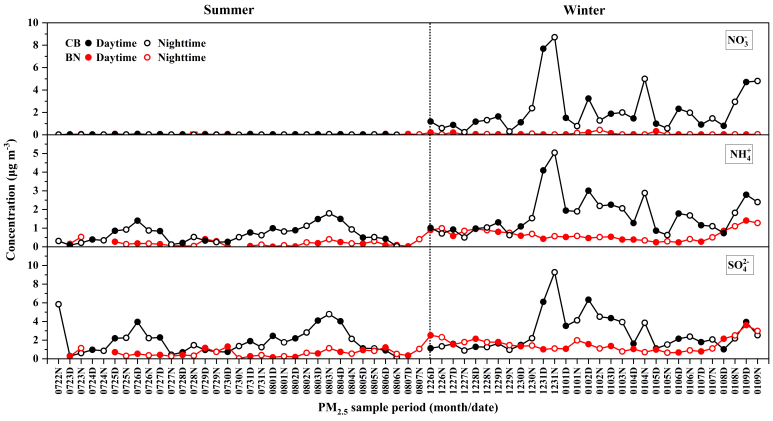

Figure 5: Temporal variations of secondary ionic species concentrations (μg m^{-3}) in PM$_{2.5}$ collected from CB and BN, China during 2023-24.

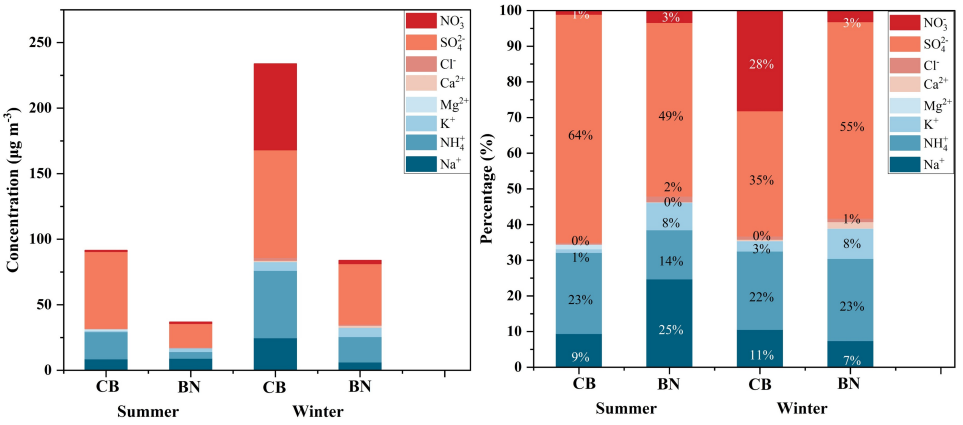

Figure 6: Concentrations and percentages of WSII in total ions.

删除了: 4

删除了: 5

删除了: s

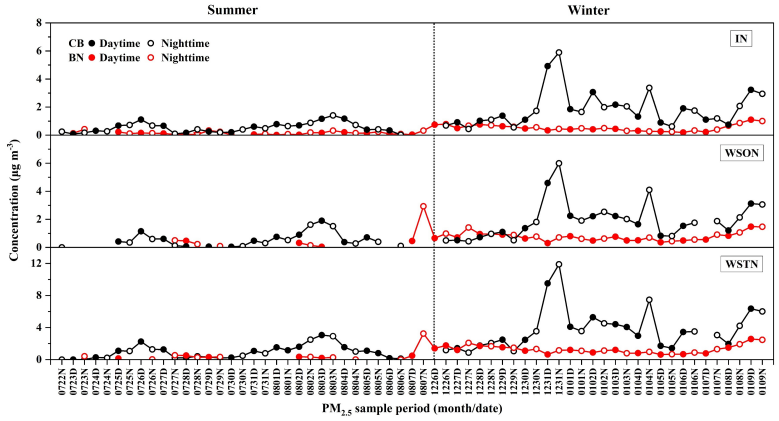

Figure 7: Temporal variations of concentrations (μg m^{-3}) of nitrogenous components in $PM_{2.5}$ collected from CB and BN, China during 2023-24.

3.2.2 Characterization of carbonaceous components and $\delta^{13}C_{TC}$

Table S1 and Figure 8 show the mass concentrations and temporal variations of OC, EC, SOC, and WSOC in $PM_{2.5}$ at CB and BN in China. The average mass concentrations of OC and EC at CB were 2.73 ± 1.72 μg m^{-3} and 0.17 ± 0.14 μg m^{-3}, while those at BN were 3.75 ± 1.33 μg m^{-3} and 0.19 ± 0.09 μg m^{-3}. Furthermore, average concentrations of OC were consistently higher than EC at both sites. OC, WSOC and SOC exhibited notable seasonal variations (Fig. 8), and their average concentrations were all higher in winter compared to summer. Overall, OC levels in winter were twice as high as in summer at both CB and BN. EC in winter were 7 times higher at CB but only 1.4 times higher at BN compared to that in summer. Elevated EC levels in winter suggested a higher influence of fossil fuel combustion. Moreover, the higher loads of OC in contrast to EC in winter and summer at both sites imply that secondary OC formation and/or increased emissions from coal combustion and biomass burning were significant. The average concentration of SOC at CB in winter (2.36 ± 1.28 μg m^{-3}) was twice as high as in summer (1.16 ± 0.60 μg m^{-3}). In addition, the average concentration of WSOC was 1.46 ± 1.00 μg m^{-3} at CB and 2.16 ± 1.03 μg m^{-3} at BN. BN exhibits a higher level of WSOC, suggesting that there might be higher emissions and/or more secondary formation occurred under conditions of greater oxidant abundance at BN than at CB. Moreover, the temporal variations of OC, WIOC, SOC, and WSOC exhibited comparable trends, suggesting a common or similar source origin and potentially similar formation processes at CB and BN.

The concentrations of OC, SOC and WSOC were higher during the daytime than at nighttime at CB and BN (Fig. 9). The intense sunlight and high temperatures prevalent in the local region might have facilitated the enhanced formation of SOC during the summer. However, EC displayed no significant diurnal variation at CB. As shown in Figure 8, OC, SOC and WSOC

删除了: 6
删除了: 7
删除了: 7
删除了: On the whole
删除了: 9
删除了: .
删除了: 7

at CB in winter showed similar diurnal trends, suggesting that they could share similar/same origins and formation processes. Elevated concentrations of carbonaceous components at CB on December 31, 2023 was observed, which could be attributed to local fireworks and firecracker celebrations in advance of the New Year's Eve. We also noticed an increase in the concentrations of OC, SOC, and WSOC in the daytime on July 30th and July 25th, 2023 at BN, which might be related to local biomass burning events.

Figure 10 illustrates the seasonal and annual variations in $\delta^{13}C_{TC}$ of CB and BN aerosols. The annual $\delta^{13}C_{TC}$ variability in $PM_{2.5}$ ranged from -27.8‰ to -22.1‰, (avg. -25.7 ± 1.5‰) at CB, while -27.6 to -24.5‰ (avg. -26.0 ± 0.9‰) at BN during the campaign. Overall, the $\delta^{13}C_{TC}$ at CB was more positive than that at BN. Compared with winter, the $\delta^{13}C_{TC}$ in summer were much lower, whose values ranged from -27.8 to -26.2‰ (avg. -27.0 ± 0.5‰) at CB, and from -27.6 to -26.2‰ (avg. -26.9 ± 0.4‰) at BN.

The diurnal variation of $\delta^{13}C_{TC}$ in the aerosols of CB and BN was not very significant, except for a slight difference in winter at CB and in summer at BN, where the average values were -24.8 ± 1.0‰ and -27.1 ± 0.3‰ at the daytime, -24.5 ± 1.2‰ and -26.7 ± 0.3‰ at the nighttime, respectively. Their values were more positive at nighttime. This might be associated with stronger plant emissions/biological activity during the daytime, and higher humidity and lower temperatures at nighttime that favored gas-to-particle transformation of organic compounds (Ren et al., 2019).

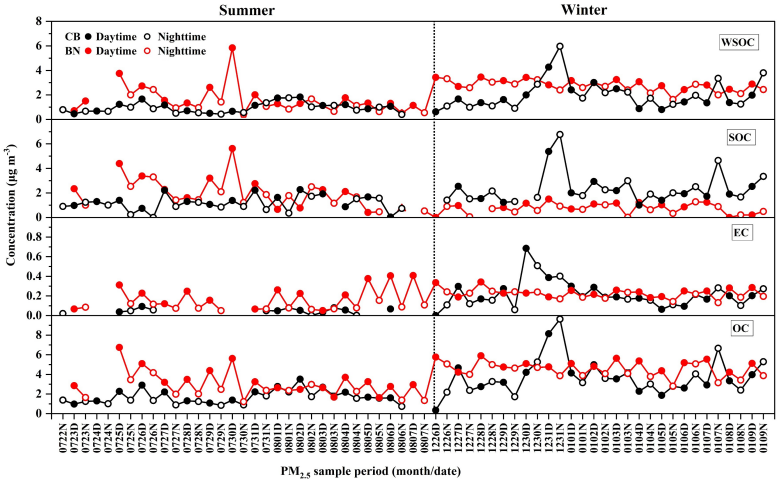

Figure 8: Temporal variations in the concentrations of OC, EC, WSOC, and SOC in $PM_{2.5}$ collected from CB and BN, China during 2023-24.

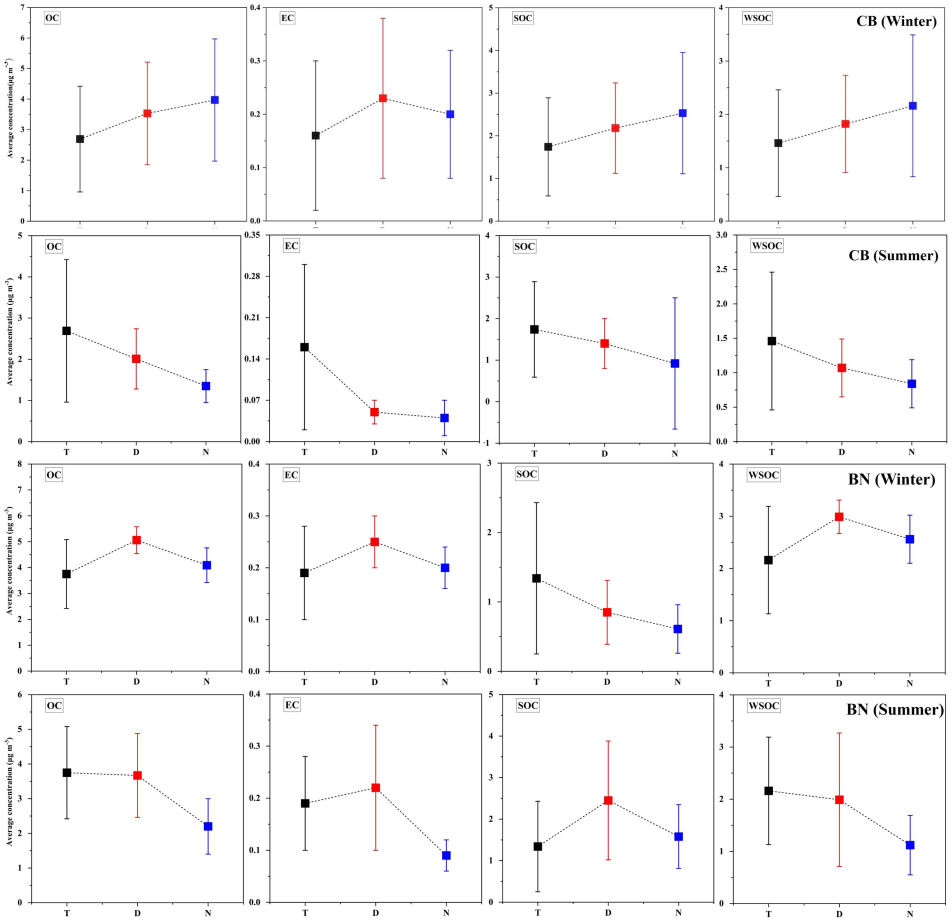

Figure 9: Diurnal variations in carbonaceous components in summer and winter forest aerosol samples collected from CB and BN, China during 2023-24. The black, red and blue squares represent the average concentrations of total (T), daytime (D) and nighttime (N).

删除了: 8

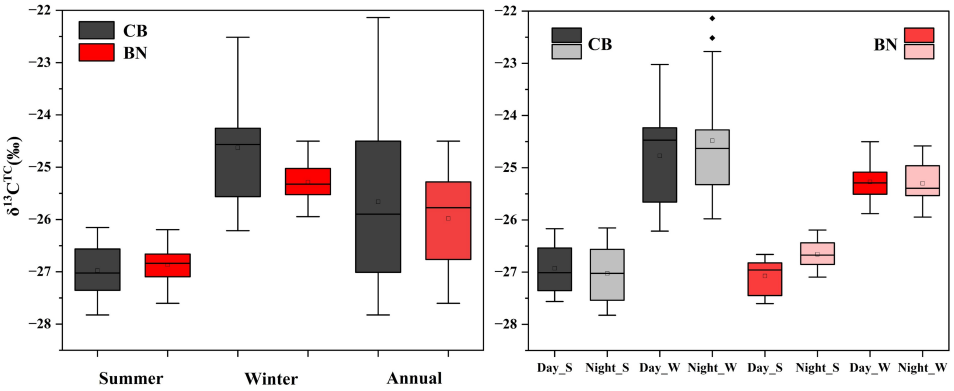

Figure 10: Seasonal and diurnal variations of $\delta^{13}C_{TC}$ collected form CB and BN during the campaign. The S and W represent summer and winter, respectively.

删除了: 9

3.3 Implications for $PM_{2.5}$ sources

3.3.1 Origins of inorganic ions

Characterization of the ionic components of aerosols from primary sources can reflect the changing characteristics of the emission sources. nss-K^+ serves as a tracer for emissions from biomass combustion, Cl^- is associated with emissions from combustion activities (coal and straw burning, etc.). However, the lower concentration of particulate Cl^- in summer may be attributed to the formation of gaseous HCl, which is volatile under high-temperature and high-humidity conditions and could escape from aerosols. The results were comparable to previously reported levels at Mt. Changbai (avg. 0.02 μg m^{-3}) and Mt. Dinghu (avg. 0.02 μg m^{-3}) (Li et al., 2010).The contributions of nss-SO_4^{2-} and nss-K^+ to the total SO_4^{2-} and K^+ concentrations were on average 87 % (summer: 78%; winter: 96%) and 85 % (summer: 76%; winter: 94%) in BN, 92 % (summer: 95%; winter: 88%) and 76 % (summer: 69%; winter: 83%) at CB, indicating a predominant influence of anthropogenic sources over marine sources, especially in winter. Since the anthropogenic sources at CB contributed more to the ions in $PM_{2.5}$, the concentration of total ions at CB was consistently higher than that at BN in both seasons, with the annual average of total ion concentration at CB being approximately 2.63 times to that at BN. There were significant correlations among SO_4^{2-}, NH_4^+, and NO_3^- at CB (Fig. 11), implying a common origin and analogous oxidation processes. The positive correlation between nss-K^+ and NO_3^-, NH_4^+, SO_4^{2-} at CB ($R^2 > 0.50$) implies that they were predominantly influenced by biomass burning.

The concentrations of secondary inorganic ions are mainly associated with the content of their gaseous precursors (SO_2, NO_x, NH_3) and the chemical reactions then undergo in the atmosphere, as well as meteorological conditions. The precursor of NO_3^- primarily originates from vehicle exhaust emissions, while the precursor of SO_4^{2-} mainly stems from coal combustion emissions from industries, residential life, and other sources. Thus, the mass ratio of NO_3^-/SO_4^{2-} can evaluate the influence of

删除了: Characterization of the ionic components of aerosols from primary sources can reflect the changing characteristics of the emission sources. nss-K^+ serves as a tracer for emissions from biomass combustion, Cl^- is associated with emissions from combustion activities (coal and straw burning, etc.) and Ca^{2+} is from crustal sources. As shown in Fig. 10, Cl^- and Mg^{2+} exhibited a relatively strong correlation (summer: $R^2 = 0.63$; winter: $R^2 = 0.51$), and had a weak correlation with Na^+ (summer: $R^2 = 0.43$) and NO_3^- (summer: $R^2 = 0.32$), indicating that Cl^- was also influenced by natural sources such as soil dust and marine sources. Ca^{2+}, as a tracer of soil and dust sources, exhibited a characteristic concentration trend with lower levels in summer and higher levels in winter at BN. It might be attributed to the scavenging effect of frequent precipitation in summer on soil and dust. Mg^{2+} exhibited a positive correlation with Ca^{2+} ($R^2 = 0.72$) during winter at BN, suggesting that Mg^{2+} might be derived from soil dust. The elevated levels of Na^+ at BN during summer were driven by marine air masses originating from the Bay of Bengal and Pacific Ocean, transported *via* southwest and southeast air currents.

设置了格式: 上标

设置了格式: 上标

删除了: as a

删除了: 10

删除了: y

mobile and stationary sources on atmospheric aerosols. The concentrations of NO_3^- were significantly low in summer at CB and BN, implying negligible contributions from motor vehicle emissions. However, the NO_3^-/SO_4^{2-} at CB in winter (0.79 ± 0.39) was approximately 26 times that in summer (0.03 ± 0.02), indicating a notable rise in the contribution of mobile sources during winter. Annual average temperature of BN was about 20℃, with a relatively large volatilization of NO_3^-, leading to a lower NO_3^-/SO_4^{2-} value (avg. 0.08 ± 0.08).

The molar ratio of NH_4^+/SO_4^{2-} in aerosols can be used to determine the acidity of aerosols and the combination form of the main secondary inorganic ions (Pathak et al., 2004; Lyu et al., 2015). When $1.5<NH_4^+/SO_4^{2-} \leq 2$, the aerosols are almost completely neutralized although ammonium nitrate is present. If $NH_4^+/SO_4^{2-}< 1.5$, the concentration of free acid in the particulate phase is relatively high, and there is almost no NH_4NO_3 present. The average ratio of NH_4^+/SO_4^{2-} at CB was 1.74 (summer: 0.97; winter: 2.54), whereas that at BN was 0.84 (summer: 0.44; winter: 1.25), suggesting an excess of ammonium existed in the aerosols at both sites, and nearly no NH_4NO_3 was present at BN. In fact, the concentrations of NO_3^- and Cl^- were extremely low at both sites in summer, so the main form of NH_4^+ were $(NH_4)_2SO_4$ and NH_4HSO_4. This resulted from elevated summer temperatures enhancing the breakdown of particulate NH_4NO_3 into gaseous NH_3 and HNO_3. SO_4^{2-} was strongly correlated with NH_4^+ at both sites, particularly in winter, which further demonstrates that $(NH_4)_2SO_4$ and NH_4HSO_4 were their primary forms. However, a favorable correlation existed between NH_4^+ and NO_3^- at CB, and the fitting slope of ammonium and $2[SO_4^{2-}] + [NO_3^-]$ in winter was greater than 1 (Fig.12), indicating that there was an adequate amount of NH_3 in the atmosphere to undergo neutralization reactions with H_2SO_4 and HNO_3, thereby forming ammonium NH_4NO_3 and $(NH_4)_2SO_4$.

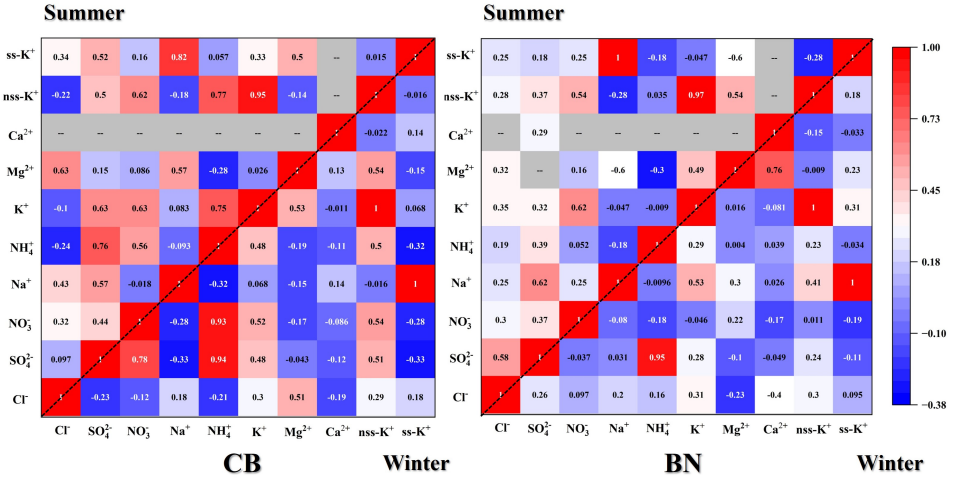

删除了：The NO_3^-/SO_4^{2-} in winter is higher than in summer, yet the average ratio remains below 1, indicating that emissions from stationary sources contribute more than those from mobile sources.

删除了：site

删除了：The lower ratio in summer at both sites, combined with the backward trajectories of air masses suggest that the air masses from ocean, rich in emissions from marine biogenic sources, might lead to a significant contribution of biogenic SO_4^{2-} in summer. Moreover, Na^+ and SO_4^{2-} at both BN ($R^2 = 0.62$) and CB ($R^2 = 0.57$) showed a moderate correlation in summer, further proving that a portion of SO_4^{2-} has come from the ocean.

删除了：1

Figure 11: Correlation heatmap of Pearson correlation coefficients of water-soluble ions.

删除了: 10

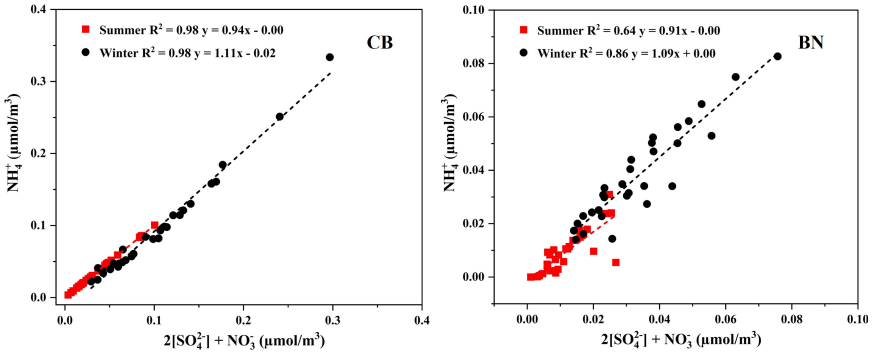

Figure 12: Linear correlations of secondary ions in $PM_{2.5}$ collected from CB and BN during the campaign period (2023-2024).

删除了: 11

3.3.2 Origins of carbonaceous components

The variation in the correlation coefficient between OC and EC was primarily affected by pollutant sources, meteorological conditions and seasonal changes. A good correlation between OC and EC suggested a single emission source, whereas a weak correlation indicated a more complex emission source. Consequently, investigating the correlation between OC and EC across different seasons can help infer the sources of carbonaceous aerosols. There were moderate correlations between OC and EC during winter at CB (R^2 = 0.46) and BN (R^2 = 0.67), but weak correlations in summer at both sites (Fig. 13). This implied that OC and EC likely shared similar sources in winter but diverged in summer.

删除了: 2

Research indicates that in the regression equation OC = aEC + b, the term "aEC" reflects primary OC emissions from combustion sources (e.g., coal and traffic), while "b" represents OC from non-combustion sources (Cao et al., 2007). The value of a at CB and BN were notably higher in winter in contrast to that in summer, implying a prominent contribution from combustion-related emissions during the winter season. The higher b value at BN in summer, implying that the impact of non-combustion source emissions was greater in summer than in winter.

删除了: *

删除了: *

删除了: *

删除了: *

The OC/EC ratios differ among various pollution sources, so the OC/EC is useful for identifying the sources and emission characteristics of carbonaceous components in $PM_{2.5}$. When the OC/EC > 2.0, it can be inferred that the secondary formation of OC is likely present (Chow et al., 2007). Studies have shown that OC/EC ratios ranging from 1.0 to 4.2 indicate traffic sources, with approximately 0.8 for heavy diesel vehicles and 2.2 for light gasoline vehicles; ratios of 2.5 to 10.5 imply coal combustion; ratios of 16.8 to 40 indicate biomass burning (Schauer et al., 1999; Chen et al., 2005). Average OC/EC ratios were 26.92 ± 16.42 at CB and 22.90 ± 9.78 at BN, which closely matched the values reported for biomass burning emissions. Table 2 showed the concentrations of OC and EC in $PM_{2.5}$ in urban and forest areas. It was not difficult to find that OC/EC in

forest areas was considerably higher than that in urban areas. The average OC/EC were 13.5 and 11.5, significantly exceeding 2.0, indicating substantial SOA formation, with higher ratios observed in summer. The elevated OC levels in summer likely resulted from the typically higher temperatures and stronger solar radiation promoted the active life activities in forest areas, which favored the emission of VOCs and thus promote the occurrence of photochemical reactions.

Table 1: Comparison of mass concentrations of OC, EC (μg m^{-3}) and OC/EC for forest aerosols over the world.

City/nation	Samling period	OC	EC	OC/EC	Reference
Look Rock, US	30 Jun.–14 Aug., 2001	5.6	0.66	8.5	(Tanner et al., 2004)
Duke Forest, US	10–23 Jul. 2003	3.2	0.2	16	(Bhat and Fraser, 2007)
K-pusta, Hungary	4 Jun.–10 Jul. 2003	4.00	0.21	19	(Kourtchev et al., 2009)
Changbai Mountain, China	Jul. 2007	4.9	0.5	9.8	(Li et al., 2010)
Chongming Island, China	Jun. 2006	9.9	1.6	6.2	
Dinghu Mountain, China	Aug. 2006	5.3	0.7	7.6	
Jiangfengling, Hainan, China	Nov. 2007	2.4	0.2	12	
Hyytiala, Finland	Jun. – Aug. 2007	1.2 ± 0.7	0.10 ± 0.06	12	(Aurela et al., 2011)
	Dec. 2007-Jan. 2008.	1.3 ± 1.2	0.24 ± 0.19	5.42	
Mt. Hua, China	Jan. 2009 Jul. -Aug. 2009	6.0 ± 2.5	0.8 ± 0.5	7.5	(Meng et al., 2014)
Baimaquan, China	18–30 Jul., 2010	15.86	1.75	9.1	(Mo et al., 2015)
Panzhihua, China	18–30 Jul., 2010	20.81	5.97	3.5	
Gongga Mountain, China	17–31 Jul., 2011	3.11	0.42	7.4	
Wolong, China	16 Jul. to 2 Aug., 2012	9.33	1.42	6.6	
Mt. Wuyi, China	2014-2015	1.6 ± 0.86	0.48 ± 0.20	3.22	(Ren et al., 2019)
		4.6 ± 1.90	0.69 ± 0.13	5.26	
Olympic Forest Park, China	2014winter	49.17 ± 15.3	7.82 ± 4.07	6.29	(Chen et al., 2020)
CB, China	2023-2024	2.73 ± 1.72	0.17 ± 0.14	26.92±16.42	This study
BN, China		3.75 ± 1.33	0.19 ± 0.09	22.90±9.78	

WSOC can be derived directly from biomass burning or form through atmospheric oxidation of VOCs (Schnelle-Kreis et al., 2007; Tang et al., 2020). When biomass burning influence is minimal, the WSOC/OC is regarded as an indicator of photochemical aging during long-range atmospheric transport. The average WSOC/OC was 0.51 ± 0.09 at CB and 0.61 ± 0.11 at BN. These results suggested that WSOC constituted a significant fraction of OC. Their range and average at CB and BN (Table S1) were comparable to those reported at urban sites, Tianjin, China (range 0.37–0.84, avg. 0.63) (Wang et al., 2018), Chennai, India (range 0.23–0.6; avg. 0.45) (Pavuluri et al., 2011a), Mt. Tai, China (0.55) (Fu et al., 2012), Gwangju, Korera (range 0.26 – 0.73, average 0.52) (Cho and Park, 2013) and Chengdu, China (avg. 0.50) (Tao et al., 2013), where biomass burning was regarded as the primary aerosol source, undergoing aging. In fact, during summer, higher temperatures and stronger solar radiation result in more vigorous plant activity in forest areas, leading to increased emissions of VOCs. Consequently, high WSOC/OC at both sites during summer were likely driven by SOA formation, linked to increased O_3 levels, solar radiation, and VOC emissions (Xiang et al., 2017). A strong correlation between WSOC and OC was found at CB (R^2 = 0.84, summer; R^2 = 0.83, winter) and BN (R^2 = 0.77, summer; R^2 = 0.75, winter), indicating that WSOC and OC share similar sources across different seasons.

SOC at CB and BN accounted for 65.2% and 38.4% of OC, respectively, and its proportions were higher in summer. The elevated SOC levels in summer likely resulted from increased atmospheric photochemical oxidation. The low SOC/OC ratio

删除了: 2

删除了: Additionally, both regions were affected by air masses which originated from the ocean during summer. These oceanic air masses were enriched with emissions from marine organisms, which subsequently undergo photochemical oxidation during long-range atmospheric transport.

(0.15) indicated that in winter at BN, the OC was mainly directly driven by local primary emissions (e.g., biomass burning, coal burning, and transportation), rather than by photochemical secondary transformation. The backward trajectory of the air mass in winter at BN further confirms that. However, SOC/OC at CB (0.57) in winter was about four times that at BN. It has been shown that biomass burning significantly increases emissions of both primary and secondary aerosols (Fu et al., 2012; Zheng et al., 2018). Specifically, these activities can enhance the formation of SOA by increasing emissions of compounds such as monoterpenes and through the action of the resultant O_3 and NOx. Thus, the high SOC/OC at CB during winter might be linked to the effective promotion of secondary aerosol formation by burning wood for heating. Furthermore, the daytime and nighttime samples collected at CB in winter exhibited diurnal variations in SOC concentrations, further confirming the significant contributions of local anthropogenic emissions and photochemical oxidation.

The WIOC fraction in the samples likely contains substantial quantities of partially combusted biogenic residues. It was noteworthy that SOC exhibited a moderate correlation with WIOC at CB ($R^2 = 0.69$; $R^2 = 0.38$), but showed no correlation at BN ($R^2 = 0.08$; $R^2 = 0.03$; Fig. 13). This implied that the source of WIOC and SOC might be similar at CB, with a significant portion of SOC being water-insoluble, while primary emissions contributed substantially at BN. The average WIOC/OC ratios at CB (0.43, summer: 0.43; winter: 0.47) and BN (summer: 0.50; winter: 0.39) were comparable to that (0.55) reported in Chennai, India, which were regarded as predominantly originating from biomass burning and undergoing aging during long-range transport (Pavuluri et al., 2011a).

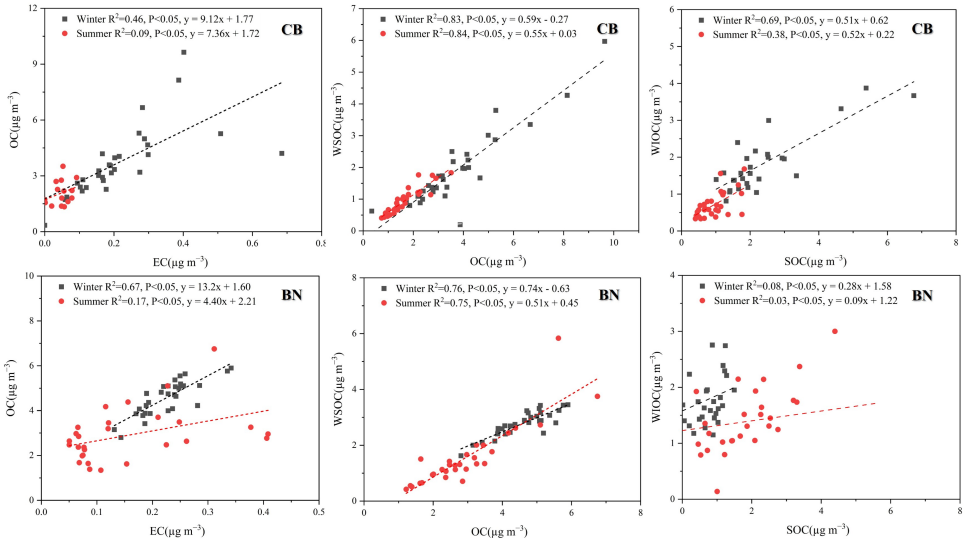

Figure 13: Correlations of certain carbonaceous components in $PM_{2.5}$ collected from CB and BN, China during 2023-24.

删除了: 2

删除了:

删除了: 12

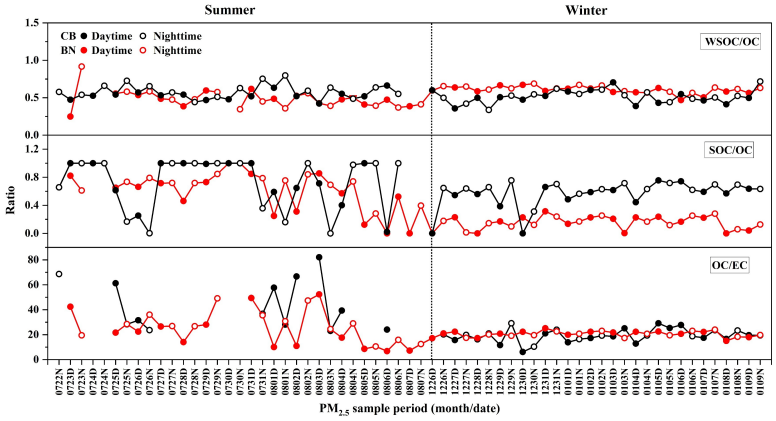

Figure 14: Temporal variations of OC/EC, WSOC/OC and SOC/OC in $PM_{2.5}$ collected from CB and BN, China during 2023-24.

删除了：13

3.3.3 Impact of biomass burning based on $\delta^{13}C_{TC}$

The aerosol particles released by plants (primary biological aerosols) exhibit a broader range. C_3 plants emit particles with $\delta^{13}C$ values ranging from -35‰ to -24‰. C_4 plants (e.g., corn, sugarcane) have $\delta^{13}C$ values in the range of -20‰ to -11‰ (Das et al., 2010; Jung and Kawamura, 2011; Mašalaitė et al., 2024). The values of $\delta^{13}C$ in summer (CB: -27.8‰ to -26.2‰; BN: -27.6‰ to -26.2‰) were significantly more negative than those in winter (CB: -26.2‰ to -22.1‰; BN: -25.9‰ to -24.5‰). This is primarily attributed to the vigorous metabolism of C_3 plants under high-temperature and high-humidity summer conditions. The Calvin cycle in plants preferentially fixes ^{12}C, resulting in ^{12}C-enriched volatile organic compounds (VOCs) such as isoprene and monoterpenes that are emitted (Hubick and Farquhar, 1989; A. Hobbie and Werner, 2004). In contrast, during winter, vegetation activity declines, and anthropogenic sources (e.g., coal combustion and biomass burning) contribute more, thereby elevating the overall isotopic ratio (Singh et al., 2018).

The $\delta^{13}C_{TC}$ observed at CB and BN during summer were comparable to those reported for aerosols in Singapore, Indonesia (-27.5 to -26.0‰) and Delhi, India (-27.7 to -24.9‰), where it was clearly indicated that the emissions from the burning of C_3 plants were the primary source of aerosols (Narukawa et al., 1999; Agarwal et al., 2024). The $\delta^{13}C$ value of aerosol derived from fossil fuel combustion was significantly higher compared to those originating from biomass burning. Moreover, Boreddy et al. (2018) had observed depletion of ^{13}C in aerosols linked to increased contributions from C_3 plant burning in Southeast Aisa and reported that photochemical aging of aerosols could have led to an increase in $\delta^{13}C_{TC}$ values (Boreddy et al., 2018). The $\delta^{13}C_{TC}$ ranged from -26.2 to -22.1‰ at CB (avg. -24.6 ± 1.1‰) and ranged from -25.9 to -24.5 at BN (avg. -25.3 ± 0.4‰)

in winter could be linked to the consumption of fossil fuels for heating and the aging of aerosols transported from continental and marine regions.

In addition, special events can also significantly affect the value of $\delta^{13}C$.On the Chinese New Year's Eve in winter at CB, significant firework - setting events were observed, resulting in a more positive $\delta^{13}C$ value on that day compared to the regular winter level (-22.8‰ vs. -26.2‰ to -22.1‰). The high temperature during the combustion of fireworks may cause the preferential volatilization of ^{12}C, leading to the enrichment of ^{13}C in the remaining particulate matter. The non - biogenic carbon from additives in fireworks may further increase the isotope ratio. Moreover, fossil fuel sources such as traffic emissions and coal - burning activities on New Year's Eve may also contribute to the isotope signal (Aguilera and Whigham, 2018).

However, no significant correlations were found between WSOC/OC and $\delta^{13}C_{TC}$ for the biomass burning aerosols, suggesting that OA at CB and BN were mostly derived from primary emissions (Cao et al., 2016). It has shown that the average values of $\delta^{13}C_{TC}$ in the remote marine aerosols ranged from -24.0 to -18.1‰ (Kawamura et al., 2017; Verwega et al., 2021). In this research, the $\delta^{13}C_{TC}$ ranged from -27.8‰ to -22.1‰ at CB and from -27.6‰ to -24.5 at BN, indicating that the contribution of marine aerosols during the campaign was relatively small. The values of $\delta^{13}C_{TC}$ in CB and BN aerosols might be the result of multiple sources' contribution, such as fossil fuel combustion (coal, natural gas and petroleum) (-28 to -21‰), marine phytoplankton (-28 to -15‰) and C_3 plants biomass burning (-28 to -26‰) (Singh et al., 2018). The concentration of SO_4^{2-} and NO_3^- at CB increased in winter, so the elevated values of $\delta^{13}C_{TC}$ were likely related to fossil fuel burning for heating. Therefore, fossil fuel combustion and C_3 plant biomass burning are identified as primary sources, while also being slightly influenced by air masses transported from the ocean during the summer.

4 Conclusions

Day- and night-time $PM_{2.5}$ samples (n = 120) were collected at two typical forest areas in North and South China. Their carbonaceous, nitrogenous, WSII, components and $\delta^{13}C_{TC}$ have been measured. The concentrations of carbonaceous and nitrogenous components displayed a distinct seasonal trend, higher in winter and lower in summer. In addition, the OC, SOC and WSOC showed diurnal variations in which their concentrations were higher during daytime than nighttime. The relationships and mass ratios of carbonaceous components indicated that the $PM_{2.5}$ at CB and BN were dominantly from biomass burning and photochemical reactions of VOCs. We also found significant deficiencies of anions in aerosols from CB and BN. Moreover, correlations between nss-K^+ and secondary ions suggested that the aerosols at two forest sites were affected by biomass burning and the primary source emissions were more important. The values of $\delta^{13}C_{TC}$ reaffirmed that biomass burning was the primary source of $PM_{2.5}$ at two sites, while they were also influenced by fossil fuel burning during winter, especially at CB, and additionally by slight oceanic air masses. Regarding the anion deficiency phenomenon found in the aerosols at the two sites in this study, we will conduct further analysis in combination with organic acids in the subsequent research to better indicate the sources and composition characteristics of aerosols in forest regions.

设置了格式: 上标

设置了格式: 上标

删除了: s

删除了: A high proportion of Na^+ was found at BN in summer, which in combination with the backward trajectory of the air mass suggested the influence of oceanic air masses.

Author contributions:

ML& ZX: Conceptualization, Investigation, Methodology, Writing–original draft. ZD: Investigation, Writing – review & editing; JD: Writing – review & editing. PF: Writing – review & editing. CMP: Funding acquisition, Writing – review & editing. ZX: Project administration, Funding acquisition, Supervision, Writing – review & editing.

Competing interests:

The authors declare that they have no conflict of interest.

Acknowledgements:

This study is supported by the National Natural Science Foundation of China Nos. 42277090 and 42202199. We appreciate Rui Liu and Jin Liu for their assistance in the field investigation.

References

A. Hobbie, E. and Werner, R. A.: Intramolecular, compound-specific, and bulk carbon isotope patterns in C3 and C4 plants: a review and synthesis, New Phytologist, 161, 371-385, 2004.

Agarwal, R., Aggarwal, S. G., Kunwar, B., Deshmukh, D. K., Singh, K., Soni, D., and Kawamura, K.: Stable isotopic, bulk, and molecular compositions of post-monsoon biomass-burning aerosols in Delhi suggest photochemical ageing during regional transport is more pronounced than local processing, Journal of Atmospheric Chemistry, 81, https://doi.org/https://doi.org/10.1007/s10874-024-09461-2, 2024.

Aggarwal, S. G., Kawamura, K., Umarji, G. S., Tachibana, E., Patil, R. S., and Gupta, P. K.: Organic and inorganic markers and stable C-, N-isotopic compositions of tropical coastal aerosols from megacity Mumbai: sources of organic aerosols and atmospheric processing, Atmos. Chem. Phys., 13, 4667-4680, https://doi.org/10.5194/acp-13-4667-2013, 2013.

Aguilera, J. and Whigham, L. D.: Using the 13C/12C carbon isotope ratio to characterise the emission sources of airborne particulate matter: a review of literature, Isotopes in Environmental and Health Studies, 54, 573-587, 2018.

Aurela, M., Saarikoski, S., Timonen, H., Aalto, P., Keronen, P., Saarnio, K., Teinilä, K., Kulmala, M., and Hillamo, R.: Carbonaceous aerosol at a forested and an urban background sites in Southern Finland, Atmospheric Environment, 45, 1394-1401, https://doi.org/https://doi.org/10.1016/j.atmosenv.2010.12.039, 2011.

Bhat, S. and Fraser, M. P.: Primary source attribution and analysis of α-pinene photooxidation products in Duke Forest, North Carolina, Atmospheric Environment, 41, 2958-2966, https://doi.org/https://doi.org/10.1016/j.atmosenv.2006.12.018, 2007.

Boreddy, S. K. R., Gogoi, M. M., Hegde, P., and Suresh Babu, S.: Chemical composition, source characteristics, and hygroscopic properties of organic-enriched aerosols in the high Arctic during summer, Science of The Total Environment, 942, 173780, https://doi.org/https://doi.org/10.1016/j.scitotenv.2024.173780, 2024.

Boreddy, S. K. R., Parvin, F., Kawamura, K., Zhu, C., and Lee, C.-T.: Stable carbon and nitrogen isotopic compositions of fine aerosols ($PM_{2.5}$) during an intensive biomass burning over Southeast Asia: Influence of SOA and aging, Atmospheric Environment, 191, 478-489, https://doi.org/https://doi.org/10.1016/j.atmosenv.2018.08.034, 2018.

Bressi, M., Sciare, J., Ghersi, V., Bonnaire, N., Nicolas, J. B., Petit, J. E., Moukhtar, S., Rosso, A., Mihalopoulos, N., and Féron, A.: A one-year comprehensive chemical characterisation of fine aerosol (PM2.5) at urban, suburban and rural background sites in the region of Paris (France), Atmos. Chem. Phys., 13, 7825-7844, https://doi.org/10.5194/acp-13-7825-2013, 2013.

Bu, X., Xie, Z., Liu, J., Wei, L., Wang, X., Chen, M., and Ren, H.: Global $PM_{2.5}$-attributable health burden from 1990 to 2017: Estimates from the Global Burden of disease study 2017, Environmental Research, 197, 111123, https://doi.org/https://doi.org/10.1016/j.envres.2021.111123, 2021.

Canaday, F. T., Georas, S. N., and Croft, D. P.: Examining the impact of air pollution, climate change, and social determinants of health on asthma and environmental justice, Current Opinion in Pulmonary Medicine, 30, 276-280, https://doi.org/10.1097/mcp.0000000000001065, 2024.

Cao, F., Zhang, S.-C., Kawamura, K., and Zhang, Y.-L.: Inorganic markers, carbonaceous components and stable carbon

设置了格式: 字体: (默认) Times New Roman

isotope from biomass burning aerosols in Northeast China, Science of The Total Environment, 572, 1244-1251, https://doi.org/https://doi.org/10.1016/j.scitotenv.2015.09.099, 2016.
Cao, J. J., Lee, S. C., Chow, J. C., Watson, J. G., Ho, K. F., Zhang, R. J., Jin, Z. D., Shen, Z. X., Chen, G. C., Kang, Y. M., Zou, S. C., Zhang, L. Z., Qi, S. H., Dai, M. H., Cheng, Y., and Hu, K.: Spatial and seasonal distributions of carbonaceous aerosols over China, Journal of Geophysical Research: Atmospheres, 112, https://doi.org/https://doi.org/10.1029/2006JD008205, 2007.
Castro, L. M., Pio, C. A., Harrison, R. M., and Smith, D. J. T.: Carbonaceous aerosol in urban and rural European atmospheres: estimation of secondary organic carbon concentrations, Atmospheric Environment, 33, 2771-2781, https://doi.org/https://doi.org/10.1016/S1352-2310(98)00331-8, 1999.
Chen, B., Liu, C., Fan, J., Shi, J., and Yu, H.: Effects of forest belt in park on the chemical composition for $PM_{2.5}$, IOP Conference Series: Earth and Environmental Science, 569, 012038, https://doi.org/10.1088/1755-1315/569/1/012038, 2020.
Chen, L., Xu, H., Huang, R., Pang, X., Wang, B., Wu, Z., and Yu, S.: Effects of nocturnal boundary layer subsidence and long-distance transports on $PM_{2.5}$ vertical profiles in the Yangtze River Delta of China measured by PM sensor on unmanned aerial vehicle and PM Lidar, Environmental Pollution, 371, 125935, https://doi.org/https://doi.org/10.1016/j.envpol.2025.125935, 2025.
Chen, S., Liu, D., Huang, L., Guo, C., Gao, X., Xu, Z., Yang, Z., Chen, Y., Li, M., and Yang, J.: Global associations between long-term exposure to $PM_{2.5}$ constituents and health: A systematic review and meta-analysis of cohort studies, Journal of Hazardous Materials, 474, 134715, https://doi.org/https://doi.org/10.1016/j.jhazmat.2024.134715, 2024.
Chen, W., Lu, X., Yuan, D., Chen, Y., Li, Z., Huang, Y., Fung, T., Sun, H., and Fung, J. C. H.: Global PM2.5 Prediction and Associated Mortality to 2100 under Different Climate Change Scenarios, Environmental Science & Technology, 57, 10039-10052, https://doi.org/10.1021/acs.est.3c03804, 2023.
Chen, Y., Sheng, G., Bi, X., Feng, Y., Mai, B., and Fu, J.: Emission Factors for Carbonaceous Particles and Polycyclic Aromatic Hydrocarbons from Residential Coal Combustion in China, Environmental Science & Technology, 39, 1861-1867, https://doi.org/10.1021/es0493650, 2005.
Cheng, M.-T., Horng, C.-L., and Lin, Y.-C.: Characteristics of atmospheric aerosol and acidic gases from urban and forest sites in central Taiwan, Bulletin of Environmental Contamination and Toxicology, 79, 674-677, 2007.
Cho, S. Y. and Park, S. S.: Resolving sources of water-soluble organic carbon in fine particulate matter measured at an urban site during winter, Environmental Science: Processes & Impacts, 15, https://doi.org/10.1039/c2em30730h, 2013.
Chow, J. C., Watson, J. G., Chen, L. W. A., Chang, M. C. O., Robinson, N. F., Trimble, D., and Kohl, S.: The IMPROVE_A temperature protocol for thermal/optical carbon analysis: maintaining consistency with a long-term database, Journal of the Air & Waste Management Association, 57, 1014-1023, 2007.
Das, O., Wang, Y., and Hsieh, Y.-P.: Chemical and carbon isotopic characteristics of ash and smoke derived from burning of C3 and C4 grasses, Organic Geochemistry, 41, 263-269, 2010.
Dong, Z., Pavuluri, C. M., Xu, Z., Wang, Y., Li, P., Fu, P., and Liu, C. Q.: Measurement report: Chemical components and ^{13}C and ^{15}N isotope ratios of fine aerosols over Tianjin, North China: year-round observations, Atmos. Chem. Phys., 23, 2119-2143, https://doi.org/10.5194/acp-23-2119-2023, 2023.
Ehn, M., Thornton, J. A., Kleist, E., Sipilä, M., Junninen, H., Pullinen, I., Springer, M., Rubach, F., Tillmann, R., Lee, B., Lopez-Hilfiker, F., Andres, S., Acir, I.-H., Rissanen, M., Jokinen, T., Schobesberger, S., Kangasluoma, J., Kontkanen, J., Nieminen, T., Kurtén, T., Nielsen, L. B., Jørgensen, S., Kjaergaard, H. G., Canagaratna, M., Maso, M. D., Berndt, T., Petäjä, T., Wahner, A., Kerminen, V.-M., Kulmala, M., Worsnop, D. R., Wildt, J., and Mentel, T. F.: A large source of low-volatility secondary organic aerosol, Nature, 506, 476-479, https://doi.org/10.1038/nature13032, 2014.
Espina-Martin, P., Perdrix, E., Alleman, L. Y., and Coddeville, P.: Origins of the seasonal variability of $PM_{2.5}$ sources in a rural site in Northern France, Atmospheric Environment, 333, 120660, https://doi.org/https://doi.org/10.1016/j.atmosenv.2024.120660, 2024.
Fu, P. Q., Kawamura, K., Chen, J., Li, J., Sun, Y. L., Liu, Y., Tachibana, E., Aggarwal, S. G., Okuzawa, K., Tanimoto, H., Kanaya, Y., and Wang, Z. F.: Diurnal variations of organic molecular tracers and stable carbon isotopic composition in atmospheric aerosols over Mt. Tai in the North China Plain: an influence of biomass burning, Atmos. Chem. Phys., 12, 8359-8375, https://doi.org/10.5194/acp-12-8359-2012, 2012.
Fu, X., Wang, X., Liu, T., He, Q., Zhang, Z., Zhang, Y., Song, W., Dai, Q., Chen, S., and Dong, F.: Secondary inorganic aerosols and aerosol acidity at different $PM_{2.5}$ pollution levels during winter haze episodes in the Sichuan Basin, China, Science of The Total Environment, 918, 170512, https://doi.org/https://doi.org/10.1016/j.scitotenv.2024.170512, 2024.

Guo, Q., Chen, K., and Xu, G.: Characteristics and Sources of Water-Soluble Inorganic Ions in $PM_{2.5}$ in Urban Nanjing, China, 10.3390/atmos14010135, 2023.
He, Q., Yan, Y., Guo, L., Zhang, Y., Zhang, G., and Wang, X.: Characterization and source analysis of water-soluble inorganic ionic species in $PM_{2.5}$ in Taiyuan city, China, Atmospheric Research, 184, 48-55, https://doi.org/10.1016/j.atmosres.2016.10.008, 2017.
Huang, R.-J., Zhang, Y., Bozzetti, C., Ho, K.-F., Cao, J.-J., Han, Y., Daellenbach, K. R., Slowik, J. G., Platt, S. M., Canonaco, F., Zotter, P., Wolf, R., Pieber, S. M., Bruns, E. A., Crippa, M., Ciarelli, G., Piazzalunga, A., Schwikowski, M., Abbaszade, G., Schnelle-Kreis, J., Zimmermann, R., An, Z., Szidat, S., Baltensperger, U., Haddad, I. E., and Prévôt, A. S. H.: High secondary aerosol contribution to particulate pollution during haze events in China, Nature, 514, 218-222, https://doi.org/10.1038/nature13774, 2014.
Hubick, K. and Farquhar, G.: Carbon isotope discrimination and photosynthesis, Annual review of plant physiology and plant molecular biology, 1989.
Jung, J. and Kawamura, K.: Springtime carbon emission episodes at the Gosan background site revealed by total carbon, stable carbon isotopic composition, and thermal characteristics of carbonaceous particles, Atmospheric Chemistry and Physics, 11, 10911-10928, 2011.
Kawamura, K., Hoque, M. M. M., Bates, T. S., and Quinn, P. K.: Molecular distributions and isotopic compositions of organic aerosols over the western North Atlantic: Dicarboxylic acids, related compounds, sugars, and secondary organic aerosol tracers, Organic Geochemistry, 113, 229-238, https://doi.org/https://doi.org/10.1016/j.orggeochem.2017.08.007, 2017.
Kawamura, K., Kobayashi, M., Tsubonuma, N., Mochida, M., Watanabe, T., and Lee, M.: Organic and inorganic compositions of marine aerosols from East Asia: Seasonal variations of water-soluble dicarboxylic acids, major ions, total carbon and nitrogen, and stable C and N isotopic composition, in: The Geochemical Society Special Publications, edited by: Hill, R. J., Leventhal, J., Aizenshtat, Z., Baedecker, M. J., Claypool, G., Eganhouse, R., Goldhaber, M., and Peters, K., Elsevier, 243-265, https://doi.org/10.1016/S1873-9881(04)80019-1, 2004.
Kawashima, H., Yoshida, O., and Suto, N.: Long-Term Source Apportionment of Ammonium in $PM_{2.5}$ at a Suburban and a Rural Site Using Stable Nitrogen Isotopes, Environmental Science & Technology, 57, 1268-1277, https://doi.org/10.1021/acs.est.2c06311, 2023.
Kourtchev, I., Copolovici, L., Claeys, M., and Maenhaut, W.: Characterization of Atmospheric Aerosols at a Forested Site in Central Europe, Environmental Science & Technology, 43, 4665-4671, https://doi.org/10.1021/es803055w, 2009.
Kunwar, B., Kawamura, K., and Zhu, C.: Stable carbon and nitrogen isotopic compositions of ambient aerosols collected from Okinawa Island in the western North Pacific Rim, an outflow region of Asian dusts and pollutants, Atmospheric Environment, 131, 243-253, https://doi.org/https://doi.org/10.1016/j.atmosenv.2016.01.035, 2016.
Lee, T., Yu, X.-Y., Kreidenweis, S. M., Malm, W. C., and Collett, J. L.: Semi-continuous measurement of PM2. 5 ionic composition at several rural locations in the United States, Atmospheric Environment, 42, 6655-6669, 2008.
Li, L., Wang, W., Feng, J., Zhang, D., Li, H., Gu, Z., Wang, B., Sheng, G., and Fu, J.: Composition, source, mass closure of $PM_{2.5}$ aerosols for four forests in eastern China, Journal of environmental sciences (China), 22, 405-412, https://doi.org/10.1016/S1001-0742(09)60122-4, 2010.
Li, Y., Wang, X., Xu, P., Gui, J., Guo, X., Yan, G., Fei, X., and Yang, A.: Chemical characterization and source identification of $PM_{2.5}$ in the Huaxi urban area of Guiyang, Scientific Reports, 14, 30451, https://doi.org/10.1038/s41598-024-81048-z, 2024.
Liou, K.-N. and Ou, S.-C.: The role of cloud microphysical processes in climate: An assessment from a one-dimensional perspective, Journal of Geophysical Research: Atmospheres, 94, 8599-8607, https://doi.org/https://doi.org/10.1029/JD094iD06p08599, 1989.
Long, Y., Zhang, W., Sun, N., Zhu, P., Yan, J., and Yin, S.: Sequential Interaction of Biogenic Volatile Organic Compounds and SOAs in Urban Forests Revealed Using Toeplitz Inverse Covariance-Based Clustering and Causal Inference, https://doi.org/10.3390/f14081617, 2023.
Lyu, X.-P., Wang, Z.-W., Cheng, H.-R., Zhang, F., Zhang, G., Wang, X.-M., Ling, Z.-H., and Wang, N.: Chemical characteristics of submicron particulates ($PM_{1.0}$) in Wuhan, Central China, Atmospheric Research, 161-162, 169-178, https://doi.org/10.1016/j.atmosres.2015.04.009, 2015.
Mace, K. A., Artaxo, P., and Duce, R. A.: Water-soluble organic nitrogen in Amazon Basin aerosols during the dry (biomass burning) and wet seasons, Journal of Geophysical Research: Atmospheres, 108, https://doi.org/https://doi.org/10.1029/2003JD003557, 2003.

Maji, K. J., Ye, W.-F., Arora, M., and Shiva Nagendra, S. M.: $PM_{2.5}$-related health and economic loss assessment for 338 Chinese cities, Environment International, 121, 392-403, https://doi.org/https://doi.org/10.1016/j.envint.2018.09.024, 2018.
Mašalaitė, A., Garbarienė, I., Garbaras, A., Šapolaitė, J., Ežerinskis, Ž., Bučinskas, L., Dudoitis, V., Kalinauskaitė, A., Pashneva, D., and Minderytė, A.: Dual-isotope ratios of carbonaceous aerosols for seasonal observation and their assessment as source indicators, Science of The Total Environment, 949, 175094, 2024.
Meinardi, S., Simpson, I. J., Blake, N. J., Blake, D. R., and Rowland, F. S.: Dimethyl disulfide (DMDS) and dimethyl sulfide (DMS) emissions from biomass burning in Australia, Geophysical research letters, 30, 2003.
Meng, J., Wang, G., Li, J., Cheng, C., Ren, Y., Huang, Y., Cheng, Y., Cao, J., and Zhang, T.: Seasonal characteristics of oxalic acid and related SOA in the free troposphere of Mt. Hua, central China: Implications for sources and formation mechanisms, Science of The Total Environment, 493, 1088-1097, https://doi.org/10.1016/j.scitotenv.2014.04.086, 2014.
Mo, H., Li, L., Lai, W., Zhao, M., Pu, J., Zhou, Y., and Deng, S.: Characterization of summer $PM_{2.5}$ aerosols from four forest areas in Sichuan, SW China, Particuology, 20, 94-103, https://doi.org/https://doi.org/10.1016/j.partic.2014.10.009, 2015.
Nah, T., Guo, H., Sullivan, A. P., Chen, Y., Tanner, D. J., Nenes, A., Russell, A., Ng, N. L., Huey, L. G., and Weber, R. J.: Characterization of aerosol composition, aerosol acidity, and organic acid partitioning at an agriculturally intensive rural southeastern US site, Atmos. Chem. Phys., 18, 11471-11491, https://doi.org/10.5194/acp-18-11471-2018, 2018.
Narukawa, M., Kawamura, K., Takeuchi, N., and Nakajima, T.: Distribution of dicarboxylic acids and carbon isotopic compositions in aerosols from 1997 Indonesian forest fires, Geophysical Research Letters, 26, 3101-3104, https://doi.org/https://doi.org/10.1029/1999GL010810, 1999.
Pathak, R. K., Louie, P. K. K., and Chan, C. K.: Characteristics of aerosol acidity in Hong Kong, Atmospheric Environment, 38, 2965-2974, https://doi.org/https://doi.org/10.1016/j.atmosenv.2004.02.044, 2004.
Pathak, R. K., Wu, W. S., and Wang, T.: Summertime $PM_{2.5}$ ionic species in four major cities of China: nitrate formation in an ammonia-deficient atmosphere, Atmos. Chem. Phys., 9, 1711-1722, https://doi.org/10.5194/acp-9-1711-2009, 2009.
Pathak, R. K., Yao, X., Lau, A. K. H., and Chan, C. K.: Acidity and concentrations of ionic species of $PM_{2.5}$ in Hong Kong, Atmospheric Environment, 37, 1113-1124, https://doi.org/https://doi.org/10.1016/S1352-2310(02)00958-5, 2003.
Pavuluri, C. M., Kawamura, K., Aggarwal, S. G., and Swaminathan, T.: Characteristics, seasonality and sources of carbonaceous and ionic components in the tropical aerosols from Indian region, Atmos. Chem. Phys., 11, 8215-8230, https://doi.org/https://dio.org/10.5194/acp-11-8215-2011, 2011a.
Pavuluri, C. M., Kawamura, K., and Fu, P. Q.: Atmospheric chemistry of nitrogenous aerosols in northeastern Asia: biological sources and secondary formation, Atmos. Chem. Phys., 15, 9883-9896, https://doi.org/10.5194/acp-15-9883-2015, 2015.
Pavuluri, C. M., Kawamura, K., Swaminathan, T., and Tachibana, E.: Stable carbon isotopic compositions of total carbon, dicarboxylic acids and glyoxylic acid in the tropical Indian aerosols: Implications for sources and photochemical processing of organic aerosols, Journal of Geophysical Research: Atmospheres, 116, https://doi.org/https://doi.org/10.1029/2011JD015617, 2011b.
Peeples, L.: How air pollution threatens brain health, Proceedings of the National Academy of Sciences, 117, 13856-13860, https://doi.org/10.1073/pnas.2008940117, 2020.
Pei, Q., Wan, X., Widory, D., Ram, K., Adhikary, B., Wu, G., Diao, X., Bhattarai, H., Zhang, Y.-L., Loewen, M., and Cong, Z.: Nitrogen aerosols in New Delhi, India: Speciation, formation, and sources, Atmospheric Research, 304, 107343, https://doi.org/https://doi.org/10.1016/j.atmosres.2024.107343, 2024.
Qiao, B., Chen, Y., Tian, M., Wang, H., Yang, F., Shi, G., Zhang, L., Peng, C., Luo, Q., and Ding, S.: Characterization of water soluble inorganic ions and their evolution processes during $PM_{2.5}$ pollution episodes in a small city in southwest China, Science of The Total Environment, 650, 2605-2613, https://doi.org/https://doi.org/10.1016/j.scitotenv.2018.09.376, 2019.
Ramana, M. V. and Devi, A.: CCN concentrations and BC warming influenced by maritime ship emitted aerosol plumes over southern Bay of Bengal, Scientific Reports, 6, 30416, https://doi.org/10.1038/srep30416, 2016.
Ren, Y., Wang, G., Tao, J., Zhang, Z., Wu, C., Wang, J., Li, J., Wei, J., Li, H., and Meng, F.: Seasonal characteristics of biogenic secondary organic aerosols at Mt. Wuyi in Southeastern China: Influence of anthropogenic pollutants, Environmental Pollution, 252, 493-500, https://doi.org/10.1016/j.envpol.2019.05.077, 2019.
Schauer, J. J., Kleeman, M. J., Cass, G. R., and Simoneit, B. R. T.: Measurement of Emissions from Air Pollution Sources. 2. C1 through C30 Organic Compounds from Medium Duty Diesel Trucks, Environmental Science & Technology, 33, 1578-1587, https://doi.org/10.1021/es980081n, 1999.
Schnelle-Kreis, J., Sklorz, M., Orasche, J., Stölzel, M., Peters, A., and Zimmermann, R.: Semi Volatile Organic Compounds

in Ambient $PM_{2.5}$. Seasonal Trends and Daily Resolved Source Contributions, Environmental Science & Technology, 41, 3821-3828, https://doi.org/10.1021/es060666e, 2007.
Sharma, S. K., Mandal, T. K., Banoo, R., Rai, A., and Rani, M.: Long-Term Variation in Carbonaceous Components of $PM_{2.5}$ from 2012 to 2021 in Delhi, Bulletin of Environmental Contamination and Toxicology, 109, 502-510, https://doi.org/10.1007/s00128-022-03506-6, 2022.
Shaughnessy, W. J., Venigalla, M. M., and Trump, D.: Health effects of ambient levels of respirable particulate matter (PM) on healthy, young-adult population, Atmospheric Environment, 123, 102-111, https://doi.org/https://doi.org/10.1016/j.atmosenv.2015.10.039, 2015.
Singh, G. K., Rajput, P., Paul, D., and Gupta, T.: Wintertime study on bulk composition and stable carbon isotope analysis of ambient aerosols from North India, Journal of Aerosol Science, 126, 231-241, https://doi.org/https://doi.org/10.1016/j.jaerosci.2018.09.010, 2018.
Sun, M. and Zhang, X.: Characteristics of $PM_{2.5}$ in Hachinohe, the priority pollution control city in Japan, Atmospheric Pollution Research, 15, 102204, https://doi.org/https://doi.org/10.1016/j.apr.2024.102204, 2024.
Tang, J., Li, J., Su, T., Han, Y., Mo, Y., Jiang, H., Cui, M., Jiang, B., Chen, Y., Tang, J., Song, J., Peng, P., and Zhang, G.: Molecular compositions and optical properties of dissolved brown carbon in biomass burning, coal combustion, and vehicle emission aerosols illuminated by excitation–emission matrix spectroscopy and Fourier transform ion cyclotron resonance mass spectrometry analysis, Atmos. Chem. Phys., 20, 2513-2532, https://doi.org/10.5194/acp-20-2513-2020, 2020.
Tanner, R. L., Parkhurst, W. J., Valente, M. L., and David Phillips, W.: Regional composition of $PM_{2.5}$ aerosols measured at urban, rural and "background" sites in the Tennessee valley, Atmospheric Environment, 38, 3143-3153, https://doi.org/https://doi.org/10.1016/j.atmosenv.2004.03.023, 2004.
Tao, J., Zhang, L., Engling, G., Zhang, R., Yang, Y., Cao, J., Zhu, C., Wang, Q., and Luo, L.: Chemical composition of $PM_{2.5}$ in an urban environment in Chengdu, China: Importance of springtime dust storms and biomass burning, Atmospheric Research, 122, 270-283, https://doi.org/10.1016/j.atmosres.2012.11.004, 2013.
Tao, Y., Yin, Z., Ye, X., Ma, Z., and Chen, J.: Size distribution of water-soluble inorganic ions in urban aerosols in Shanghai, Atmospheric Pollution Research, 5, 639-647, https://doi.org/https://doi.org/10.5094/APR.2014.073, 2014.
Tian, S., Pan, Y., and Wang, Y.: Ion balance and acidity of size-segregated particles during haze episodes in urban Beijing, Atmospheric Research, 201, 159-167, 2018.
Tripathee, L., Kang, S., Chen, P., Bhattarai, H., Guo, J., Shrestha, K. L., Sharma, C. M., Sharma Ghimire, P., and Huang, J.: Water-soluble organic and inorganic nitrogen in ambient aerosols over the Himalayan middle hills: Seasonality, sources, and transport pathways, Atmospheric Research, 250, https://doi.org/10.1016/j.atmosres.2020.105376, 2021.
Tripathee, L., Kang, S., Rupakheti, D., Cong, Z., Zhang, Q., and Huang, J.: Chemical characteristics of soluble aerosols over the central Himalayas: insights into spatiotemporal variations and sources, Environmental Science and Pollution Research, 24, 24454-24472, 2017.
Verwega, M. T., Somes, C. J., Schartau, M., Tuerena, R. E., Lorrain, A., Oschlies, A., and Slawig, T.: Description of a global marine particulate organic carbon-13 isotope data set, Earth Syst. Sci. Data, 13, 4861-4880, https://doi.org/10.5194/essd-13-4861-2021, 2021.
Wan, X., Kang, S., Li, Q., Rupakheti, D., Zhang, Q., Guo, J., Chen, P., Tripathee, L., Rupakheti, M., Panday, A. K., Wang, W., Kawamura, K., Gao, S., Wu, G., and Cong, Z.: Organic molecular tracers in the atmospheric aerosols from Lumbini, Nepal, in the northern Indo-Gangetic Plain: influence of biomass burning, Atmos. Chem. Phys., 17, 8867–8885, https://doi.org/10.5194/acp-17-8867-2017, 2017.
Wan, X., Kang, S., Wang, Y., Xin, J., Liu, B., Guo, Y., Wen, T., Zhang, G., and Cong, Z.: Size distribution of carbonaceous aerosols at a high-altitude site on the central Tibetan Plateau (Nam Co Station, 4730 m a.s.l.), Atmos. Res., 153, 155–164, https://doi.org/10.1016/j.atmosres.2014.08.008, 2015.
Wang, B., Li, Y., Tang, Z., and Cai, N.: The carbon components in indoor and outdoor $PM_{2.5}$ in winter of Tianjin, Scientific Reports, 11, 17881, https://doi.org/10.1038/s41598-021-97530-x, 2021.
Wang, Q., Jiang, N., Yin, S., Li, X., Yu, F., Guo, Y., and Zhang, R.: Carbonaceous species in $PM_{2.5}$ and PM_{10} in urban area of Zhengzhou in China: Seasonal variations and source apportionment, Atmospheric Research, 191, 1-11, https://doi.org/https://doi.org/10.1016/j.atmosres.2017.02.003, 2017.
Wang, S., Pavuluri, C. M., Ren, L., Fu, P., Zhang, Y.-L., and Liu, C.-Q.: Implications for biomass/coal combustion emissions and secondary formation of carbonaceous aerosols in North China, RSC Advances, 8, 38108-38117,

设置了格式: 字体: (默认) Times New Roman

https://doi.org/10.1039/C8RA06127K, 2018.
Wang, Y., Zhang, X., Arimoto, R., Cao, J., and Shen, Z.: Characteristics of carbonate content and carbon and oxygen isotopic composition of northern China soil and dust aerosol and its application to tracing dust sources, Atmospheric Environment, 39, 2631-2642, https://doi.org/10.1016/j.atmosenv.2005.01.015, 2005.
Wu Wenlu, Chen Haisha, Guo Jianping, Xu Zhiqi and Zhang Xiaoyan: Regionalization of the Boundary-Layer Height and its Dominant Influence Factors in Summer over China [J]. Chinese Journal of Atmospheric Sciences (in Chinese), 48, 1201-1216, https://doi.org/10.3878/j.issn.1006-9895.2212.22183, 2024.
Wu, K., Yang, X., Chen, D., Gu, S., Lu, Y., Jiang, Q., Wang, K., Ou, Y., Qian, Y., Shao, P., and Lu, S.: Estimation of biogenic VOC emissions and their corresponding impact on ozone and secondary organic aerosol formation in China, Atmospheric Research, 231, https://doi.org/10.1016/j.atmosres.2019.104656, 2020.
Xiang, P., Zhou, X., Duan, J., Tan, J., He, K., Yuan, C., Ma, Y., and Zhang, Y.: Chemical characteristics of water-soluble organic compounds (WSOC) in $PM_{2.5}$ in Beijing, China: 2011–2012, Atmospheric Research, 183, 104-112, https://doi.org/10.1016/j.atmosres.2016.08.020, 2017.
Xue, B., Kuang, Y., Xu, W., and Zhao, P.: Joint increase of aerosol scattering efficiency and aerosol hygroscopicity aggravate visibility impairment in the North China Plain, Science of The Total Environment, 839, 156279, https://doi.org/https://doi.org/10.1016/j.scitotenv.2022.156279, 2022.
Yin, H., McDuffie, E. E., Martin, R. V., and Brauer, M.: Global health costs of ambient $PM_{2.5}$ from combustion sources: a modelling study supporting air pollution control strategies, The Lancet Planetary Health, 8, e476-e488, https://doi.org/10.1016/S2542-5196(24)00098-6, 2024.
Yin, L., Niu, Z., Chen, X., Chen, J., Zhang, F., and Xu, L.: Characteristics of water-soluble inorganic ions in $PM_{2.5}$ and PM2.5–10 in the coastal urban agglomeration along the Western Taiwan Strait Region, China, Environmental Science and Pollution Research, 21, 5141-5156, https://doi.org/10.1007/s11356-013-2134-7, 2014.
Yuan, B., Hu, W. W., Shao, M., Wang, M., Chen, W. T., Lu, S. H., Zeng, L. M., and Hu, M.: VOC emissions, evolutions and contributions to SOA formation at a receptor site in eastern China, Atmos. Chem. Phys., 13, 8815-8832, https://doi.org/10.5194/acp-13-8815-2013, 2013.
Zhang, Z., Shao, C., Guan, Y., and Xue, C.: Socioeconomic factors and regional differences of $PM_{2.5}$ health risks in China, Journal of Environmental Management, 251, 109564, https://doi.org/https://doi.org/10.1016/j.jenvman.2019.109564, 2019.
Zhang, Z., Zeng, Y., Zheng, N., Luo, L., Xiao, H., and Xiao, H.: Fossil fuel-related emissions were the major source of NH_3 pollution in urban cities of northern China in the autumn of 2017, Environmental Pollution, 256, 113428, https://doi.org/https://doi.org/10.1016/j.envpol.2019.113428, 2020.
Zhao, X., Xu, Z., Li, P., Dong, Z., Fu, P., Liu, C.-Q., and Pavuluri, C. M.: Characteristics and seasonality of trace elements in fine aerosols from Tianjin, North China during 2018-2019, Environmental Advances, 9, 100263, https://doi.org/https://doi.org/10.1016/j.envadv.2022.100263, 2022.
Zheng, L., Yang, X., Lai, S., Ren, H., Yue, S., Zhang, Y., Huang, X., Gao, Y., Sun, Y., Wang, Z., and Fu, P.: Impacts of springtime biomass burning in the northern Southeast Asia on marine organic aerosols over the Gulf of Tonkin, China, Environmental Pollution, 237, 285-297, https://doi.org/10.1016/j.envpol.2018.01.089, 2018.
Zheng, M., Wang, Y., Yuan, L., Chen, N., and Kong, S.: Ambient observations indicating an increasing effectiveness of ammonia control in wintertime $PM_{2.5}$ reduction in Central China, Science of The Total Environment, 824, 153708, https://doi.org/https://doi.org/10.1016/j.scitotenv.2022.153708, 2022.
Zheng, Z., Chen, L., Sun, N., Jin, Y., and Wang, Y.: Pollution, hazards, and health inequalities: a longitudinal exploration of the impact of $PM_{2.5}$ on depression among rural older adults with different incomes in China, Humanities and Social Sciences Communications, 11, 1682, https://doi.org/10.1057/s41599-024-04233-5, 2024.

删除了：

删除了：

删除了：Tian, S., Pan, Y., and Wang, Y.: Ion balance and acidity of size-segregated particles during haze episodes in urban Beijing, Atmospheric Research, 201, 159-167, 2018.

第 5 页: [1] 设置了格式 Xu Zhan-Jie 2025/7/3 11:32:00

字体: +西文正文 (Times New Roman), 非突出显示

第 5 页: [1] 设置了格式 Xu Zhan-Jie 2025/7/3 11:32:00

字体: +西文正文 (Times New Roman), 非突出显示

第 5 页: [1] 设置了格式 Xu Zhan-Jie 2025/7/3 11:32:00

字体: +西文正文 (Times New Roman), 非突出显示

第 5 页: [2] 设置了格式 Xu Zhan-Jie 2025/7/3 11:32:00

字体: (默认) +西文正文 (Times New Roman), 非突出显示

第 5 页: [2] 设置了格式 Xu Zhan-Jie 2025/7/3 11:32:00

字体: (默认) +西文正文 (Times New Roman), 非突出显示

第 5 页: [2] 设置了格式 Xu Zhan-Jie 2025/7/3 11:32:00

字体: (默认) +西文正文 (Times New Roman), 非突出显示

第 5 页: [3] 设置了格式 Xu Zhan-Jie 2025/7/3 11:32:00

字体: (默认) +西文正文 (Times New Roman), 非突出显示

第 5 页: [3] 设置了格式 Xu Zhan-Jie 2025/7/3 11:32:00

字体: (默认) +西文正文 (Times New Roman), 非突出显示

第 5 页: [3] 设置了格式 Xu Zhan-Jie 2025/7/3 11:32:00

字体: (默认) +西文正文 (Times New Roman), 非突出显示

第 5 页: [4] 设置了格式 Xu Zhan-Jie 2025/7/3 11:07:00

字体: (默认) +西文正文 (Times New Roman)

第 5 页: [4] 设置了格式 Xu Zhan-Jie 2025/7/3 11:07:00

字体: (默认) +西文正文 (Times New Roman)

第 5 页: [4] 设置了格式 Xu Zhan-Jie 2025/7/3 11:07:00

字体: (默认) +西文正文 (Times New Roman)

第 5 页: [5] 设置了格式 Xu Zhan-Jie 2025/7/3 11:08:00

字体: +西文正文 (Times New Roman)

第 5 页: [5] 设置了格式 Xu Zhan-Jie 2025/7/3 11:08:00

字体: +西文正文 (Times New Roman)

第 5 页: [5] 设置了格式 Xu Zhan-Jie 2025/7/3 11:08:00

字体: +西文正文 (Times New Roman)

第 5 页: [6] 设置了格式 Xu Zhan-Jie 2025/7/3 11:08:00

字体: (默认) +西文正文 (Times New Roman)

第 5 页: [6] 设置了格式 Xu Zhan-Jie 2025/7/3 11:08:00

字体: (默认) +西文正文 (Times New Roman)

第 5 页: [6] 设置了格式 Xu Zhan-Jie 2025/7/3 11:08:00

字体: (默认) +西文正文 (Times New Roman)

第 5 页: [7] 设置了格式 Xu Zhan-Jie 2025/7/3 11:08:00

字体: (默认) +西文正文 (Times New Roman)

第 5 页: [7] 设置了格式 Xu Zhan-Jie 2025/7/3 11:08:00

字体: (默认) +西文正文 (Times New Roman)

第 5 页: [7] 设置了格式 Xu Zhan-Jie 2025/7/3 11:08:00

字体: (默认) +西文正文 (Times New Roman)

第 5 页: [8] 设置了格式 Xu Zhan-Jie 2025/7/3 11:09:00

字体: (默认) +西文正文 (Times New Roman)

第 5 页: [8] 设置了格式 Xu Zhan-Jie 2025/7/3 11:09:00

字体: (默认) +西文正文 (Times New Roman)

第 5 页: [8] 设置了格式 Xu Zhan-Jie 2025/7/3 11:09:00

字体: (默认) +西文正文 (Times New Roman)

第 5 页: [9] 设置了格式 Xu Zhan-Jie 2025/7/3 11:09:00

字体: (默认) +西文正文 (Times New Roman)

第 5 页: [9] 设置了格式 Xu Zhan-Jie 2025/7/3 11:09:00

字体: (默认) +西文正文 (Times New Roman)

第 5 页: [9] 设置了格式 Xu Zhan-Jie 2025/7/3 11:09:00

字体: (默认) +西文正文 (Times New Roman)

第 5 页: [10] 删除了 Xu Zhan-Jie 2025/6/19 20:36:00

第 5 页: [10] 删除了 Xu Zhan-Jie 2025/6/19 20:36:00

第 8 页: [11] 删除了 明宇 李 2025/6/21 21:31:00

第 8 页: [11] 删除了 明宇 李 2025/6/21 21:31:00

第 8 页: [12] 设置了格式 Xu Zhan-Jie 2025/7/3 11:10:00

字体: (默认) +西文正文 (Times New Roman)

第 8 页: [12] 设置了格式 Xu Zhan-Jie 2025/7/3 11:10:00

字体: (默认) +西文正文 (Times New Roman)

第 8 页: [12] 设置了格式 Xu Zhan-Jie 2025/7/3 11:10:00

字体: (默认) +西文正文 (Times New Roman)

第 8 页: [12] 设置了格式 Xu Zhan-Jie 2025/7/3 11:10:00

字体: (默认) +西文正文 (Times New Roman)

第 8 页: [13] 设置了格式 Xu Zhan-Jie 2025/7/3 11:10:00

字体: (默认) +西文正文 (Times New Roman)

第 8 页: [13] 设置了格式 Xu Zhan-Jie 2025/7/3 11:10:00

字体: (默认) +西文正文 (Times New Roman)

第 8 页: [13] 设置了格式 Xu Zhan-Jie 2025/7/3 11:10:00

字体: (默认) +西文正文 (Times New Roman)

第 8 页: [13] 设置了格式 Xu Zhan-Jie 2025/7/3 11:10:00

字体: (默认) +西文正文 (Times New Roman)

第 8 页: [14] 设置了格式 Xu Zhan-Jie 2025/7/3 11:10:00

字体: Times New Roman

第 8 页: [14] 设置了格式 Xu Zhan-Jie 2025/7/3 11:10:00

字体: Times New Roman

第 8 页: [14] 设置了格式 Xu Zhan-Jie 2025/7/3 11:10:00

字体: Times New Roman

第 8 页: [14] 设置了格式 Xu Zhan-Jie 2025/7/3 11:10:00

字体: Times New Roman

第 8 页: [14] 设置了格式 Xu Zhan-Jie 2025/7/3 11:10:00

字体: Times New Roman

第 8 页: [15] 设置了格式 Xu Zhan-Jie 2025/7/3 11:10:00

字体: (默认) +西文正文 (Times New Roman)

第 8 页: [15] 设置了格式 Xu Zhan-Jie 2025/7/3 11:10:00

字体: (默认) +西文正文 (Times New Roman)

第 8 页: [15] 设置了格式 Xu Zhan-Jie 2025/7/3 11:10:00

字体: (默认) +西文正文 (Times New Roman)

第 8 页: [15] 设置了格式 Xu Zhan-Jie 2025/7/3 11:10:00

字体: (默认) +西文正文 (Times New Roman)

第 8 页: [16] 设置了格式 Xu Zhan-Jie 2025/7/3 11:20:00

字体: (默认) +西文正文 (Times New Roman)

第 8 页: [16] 设置了格式 Xu Zhan-Jie 2025/7/3 11:20:00

字体: (默认) +西文正文 (Times New Roman)

第 8 页: [16] 设置了格式 Xu Zhan-Jie 2025/7/3 11:20:00

字体: (默认) +西文正文 (Times New Roman)

第 8 页: [16] 设置了格式 Xu Zhan-Jie 2025/7/3 11:20:00

字体: (默认) +西文正文 (Times New Roman)

第 8 页: [16] 设置了格式 Xu Zhan-Jie 2025/7/3 11:20:00

字体: (默认) +西文正文 (Times New Roman)

第 8 页: [17] 设置了格式 Xu Zhan-Jie 2025/7/3 11:21:00

字体: (默认) +西文正文 (Times New Roman)

第 8 页: [17] 设置了格式 Xu Zhan-Jie 2025/7/3 11:21:00

字体: (默认) +西文正文 (Times New Roman)

第 8 页: [17] 设置了格式 Xu Zhan-Jie 2025/7/3 11:21:00

字体: (默认) +西文正文 (Times New Roman)

第 8 页: [18] 设置了格式 Xu Zhan-Jie 2025/7/3 11:21:00

字体: (默认) +西文正文 (Times New Roman)

第 8 页: [18] 设置了格式 Xu Zhan-Jie 2025/7/3 11:21:00

字体: (默认) +西文正文 (Times New Roman)

第 8 页: [19] 设置了格式 Xu Zhan-Jie 2025/7/3 11:22:00

字体: (默认) +西文正文 (Times New Roman)

第 8 页: [19] 设置了格式 Xu Zhan-Jie 2025/7/3 11:22:00

字体: (默认) +西文正文 (Times New Roman)

第 8 页: [20] 删除了 明宇 李 2025/6/23 09:18:00

第 8 页: [20] 删除了 明宇 李 2025/6/23 09:18:00

第 8 页: [21] 设置了格式 Xu Zhan-Jie 2025/7/3 11:23:00

字体: (默认) +西文正文 (Times New Roman)

第 8 页: [21] 设置了格式 Xu Zhan-Jie 2025/7/3 11:23:00

字体: (默认) +西文正文 (Times New Roman)

第 8 页: [21] 设置了格式 Xu Zhan-Jie 2025/7/3 11:23:00

字体: (默认) +西文正文 (Times New Roman)

第 8 页: [22] 设置了格式 Xu Zhan-Jie 2025/7/3 11:23:00

字体: (默认) +西文正文 (Times New Roman)

第 8 页: [22] 设置了格式 Xu Zhan-Jie 2025/7/3 11:23:00

字体: (默认) +西文正文 (Times New Roman)

第 8 页: [22] 设置了格式 Xu Zhan-Jie 2025/7/3 11:23:00

字体: (默认) +西文正文 (Times New Roman)

第 8 页: [23] 删除了 明宇 李 2025/6/23 10:38:00

第 8 页: [23] 删除了 明宇 李 2025/6/23 10:38:00

第 8 页: [23] 删除了 明宇 李 2025/6/23 10:38:00

第 8 页: [23] 删除了 明宇 李 2025/6/23 10:38:00

第 8 页: [23] 删除了 明宇 李 2025/6/23 10:38:00

第 8 页: [23] 删除了 明宇 李 2025/6/23 10:38:00

第 8 页: [23] 删除了 明宇 李 2025/6/23 10:38:00

第 10 页: [24] 删除了 明宇 李 2025/6/25 14:25:00